Cover Page

INTERNATIONAL JOURNAL OF MULTIDISCIPLINARY EDUCATIONAL RESEARCH
ISSN:2277-7881(Print); IMPACT FACTOR :9.014(2025); IC VALUE:5.16; ISI VALUE:2.286
PEER REVIEWED AND REFEREED INTERNATIONAL JOURNAL
(Fulfilled Suggests Parameters of UGC by IJMER)
Volume:14, Issue:8(1), August, 2025
Scopus Review ID: A2B96D3ACF3FEA2A
Article Received: Reviewed : Accepted
Publisher: Sucharitha Publication, India
Online Copy of Article Publication Available : www.ijmer.in
https://doi.org/ijmer.in/14.08(1)/2025.33

The exploration of the double dispersion effect and exothermic chemical reaction on thermally radiating hydromagnetic convective heat and mass transfer flow involving tetra, ternary, and hybrid nanofluids (Al_2O_3 + Cu + SiO_2 + TiO_2/Eg) over a stretching sheet with multiple slips

H.G. Suguna
Associate Professor, Department of Mathematics, GFGC, Sidlaghatta
Chikkaballapur (Dt), Karnataka, India
sugunareddy.srinivas@gmail.com, Mobile : +91 9880674100
ORCID: https://orcid.org/0000-0002-0047-392X

Abstract :

This study investigates the combined effects of double dispersion (Thermal & Solutal parameters (Ds & Dc)), exothermic chemical reaction, thermal radiation, and magnetic field on the convective heat and mass transfer flow of ethylene glycol-based tetra, ternary, and hybrid nanofluids comprising Al_2O_3, Cu, SiO_2, and TiO_2 nanoparticles over a stretching sheet with multiple slip conditions. The governing nonlinear partial differential equations describing momentum, energy, and concentration transport are transformed into a system of ordinary differential equations using with using RKF-45 numerical approach and similarity transformations and solved numerically. The influences of key physical parameters, including magnetic field strength, thermal radiation, velocity slip, thermal slip, solutal slip, exothermic reaction, and nanoparticle volume fraction, on Velocity(f'), temperature(θ) and nanoconcentration (Φ) distributions are analyzed have been shown graphically for different parametric variation. It is found that Increasing Thermal dispersion parameter (Ds) improves boundary layer velocity profile. Ds increases boundary layer fluid temperature by diffusing thermal energy from hotter to cooler locations. Tetra nanofluids outperform ternary and hybrid nanofluids in f', θ & Φ. An increase in solutal dispersion parameter (Dc) leads to an enhancement in the velocity profile. The temperature profile increases with increasing Dc Higher solutal dispersion promotes species transport and reduces concentration gradients. This shows that adding nanoparticles to ethylene glycol-based nanofluids increases heat and mass transmission(Ds & Dc). Velocity enhances with reduces with radiation(Q1). θ enhances with Q1 in all types of nanofluids.Φ grows with Q1. τ, Nu grows with Q1 at η=0. Sh reduces with increase in Q1 in all types of nanofluids.

Keywords : Tetra, Ternary and Hybrid(AlO2- Cu- SiO2-TiO2) nanofluid, double dispersion, exothermic chemical reaction, heat and mass transfer, Stretching sheet, Activation energy, multiple slips.

1. INTRODUCTION

1.1. Double Dispersion

Hydrodynamic mixing, referred to as dispersion, is a secondary impact of a porous medium on fluid flow, resulting from the mixing and cycling of local fluid particles through the convoluted pathways created by the solid particles of the porous medium. Renewed interest in the study of double diffusive convection has emerged due to the influence of thermal and solutal dispersions, which represent supplementary processes of energy and concentration mass movement. In specific thermal and solutal dispersion applications, including oil reservoir and geothermal engineering, as well as ceramic processing, sensible heat storage beds, and petroleum recovery. A concise examination of double dispersion effects, encompassing thermal and solutal dispersion, is available in Bear [1] and Nield and Bejan [2]. Kvernold and Tyvand [3] examined heat dispersion effects and identified a closer alignment between the experimental and theoretical findings. The examination of thermal and solutal dispersion is extensively addressed in the works of Cheng [4], Telles and Trevisan [5], Hassanien et al. [6], El-Hakiem [7], Chamkha et al. [8], and Khaled and Vafai [9]. Ibrhim et al. [10], Mallikarjuna [11], and Slattery [12] examined the effects of thermal and solutal dispersion on Darcy and non-Darcy convective heat and mass transfer flows across various geometries in a porous media. Kristaiah Pallala [13] has examined the impact of double dispersion on hydromagnetic convective heat and mass transfer flow adjacent to a vertical wavy wall, incorporating variable viscosity, thermal conductivity, thermal radiation, and temperature-dependent heat sources. Srinivasa Reddy and Ranganatha Reddy [14] have investigated the impact of double dispersion on convective heat and mass transfer flow across a vertical wavy surface with non-uniform heat sources. Srinivasacharya et al. [15-17] investigated variable properties and cross-diffusion effects on mixed convective flow over a vertical wavy surface in a fluid-saturated porous medium, and also examined dispersion effects on mixed convection over a vertical wavy surface in a porous medium with variable properties. Amitosh Tiwari and colleagues have recently conducted a study on the numerical analysis of dispersion and activation energy in convective heat transfer flow over a wavy surface with variable properties and heat sources.

Cover Page

INTERNATIONAL JOURNAL OF MULTIDISCIPLINARY EDUCATIONAL RESEARCH
ISSN:2277-7881(Print); IMPACT FACTOR :9.014(2025); IC VALUE:5.16; ISI VALUE:2.286
PEER REVIEWED AND REFEREED INTERNATIONAL JOURNAL
(Fulfilled Suggests Parameters of UGC by IJMER)
Volume:14, Issue:8(1), August, 2025
Scopus Review ID: A2B96D3ACF3FEA2A
Article Received: Reviewed : Accepted
Publisher: Sucharitha Publication, India
Online Copy of Article Publication Available : www.ijmer.in
https://doi.org/ijmer.in/14.08(1)/2025.33

1.2. Activation energy & Exothermic chemical reaction

The activation energy is responsible for both Arrhenius-type temperature change and the synergistic, structural, and morphological effects of the multi-component nanoparticle network. To accurately record temperature variations, researchers may employ "modified Arrhenius functions" or incorporate adjustment variables for clustering, volume percentage, slip, and so on. Several authors have researched hall effects using Arrhenius activation energy, including Krishna et al. Netai Roy and Dulal Pal [19] investigated how activation energy, radiation, nonlinear thermal radiation, and ohmic dissipation affect Casson nanofluid heat and mass transmission over a stretched sheet.

A chemical process alters the quantity and composition of its constituents. When the chemical relationship between atoms is broken, just their interior structures pass through. The type of reaction is one of the most critical elements in determining how quickly a chemical reaction occurs. The chemical process is critical for enhancing heat transfer through normal fluids. Chemical processes move mass and heat, which can be employed in the industrial sector to perform critical engineering tasks such as drying, temperature control, and moisture distribution. There are two types of chemical reactions: exothermic and endothermic. When a process produces heat yet alters enthalpy negatively, this is referred to as an exothermic reaction. Because of this, many chemical processes emit sound, light, or heat. Chemical reactions and activation energy have numerous applications, including food preparation, chemical engineering, oil emulsions, and geothermal reserves. Several researchers (Krishna et al. [20], Devasena [21], Kathyani and Subramanyam [22], Nagasasikala [23], Satya Narayana and Ramakrishna [24], Obalalu et al. [25-27], and Adeshina et al. [28]) investigated the hall effects for chemical processes with MHD flow and a fixed Arrhenius activation energy.

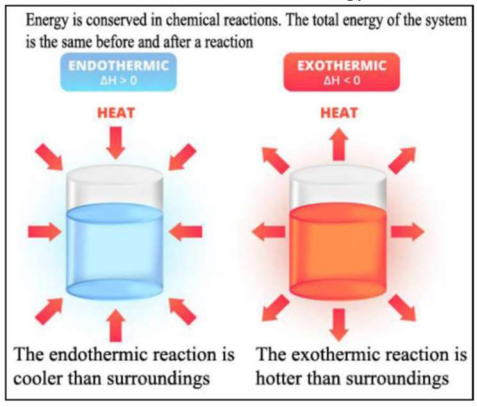


Fig.1a. Chemical reactions with exothermic and endothermic.

1.3. Tetra & Hybrid Nanofluid

A nanofluid is a mixture that has nanoparticles distributed throughout a base fluid such as water or ethylene glycol. The adjustments to the base fluid improve its viscosity, thermal conductivity, and other properties. Jan et al. [29] investigated the convective dynamics and heat transfer of a non-Newtonian nanofluid with Reiner-Philippoff viscosity and a homogeneous model moving across a curved stretched surface with magnetic effects. Tetra-hybrid nanofluids are created by dispersing four different types of nanoparticles into a base fluid. They have garnered significant attention due to their improved thermal and flow properties when compared to mono- or hybrid nanofluids. Tetra-hybrid nanofluids provide improved thermal and flow properties that are useful in a variety of everyday applications. The combined effects improve thermal conductivity, convective heat transfer, and energy transport efficiency. These properties make them suitable for use in vehicle cooling systems, HVAC units, solar collectors, and electronic cooling. These fluids also have variable viscosity, enhanced stability, and better dispersion, making them suitable for application in biomedical devices, microfluidics, and heat storage systems. Ramadhan et al. [30] explained how tri-hybrid nanofluids increase thermal conductivity in a water-ethylene glycol base. Vedavathi et al. [31] presented a review report highlighting the entropy behavior in MHD convection past an inclined surface. Guedri et al. [32] investigated the behavior of a radiative nanofluid exposed to the Darcy-Forchheimer effect on a nonlinear stretching surface. These cutting-edge fluids are critical for significant improvement, as seen in Fig. 1a (Applications) and Fig. 1b (Procedure flow chart). Abbas et al. [33] investigated tetra hybrid nanofluid around a vertical cylinder, taking into account the effects of magnetic field and thermal conductivity. Chamkha et al. [34], Gul and Saeed [35], and Sajid et al. [36] investigated the effects of an angled magnetic field and heat generation on the flow of a cross-tetra hybrid nanofluid over a wedge during homogeneous/heterogeneous chemical processes. Both investigations found that tetra-hybrid nanofluid had better heat transfer capability than tri-hybrid and hybrid nanofluid.

Cover Page

INTERNATIONAL JOURNAL OF MULTIDISCIPLINARY EDUCATIONAL RESEARCH
ISSN:2277-7881(Print); IMPACT FACTOR :9.014(2025); IC VALUE:5.16; ISI VALUE:2.286
PEER REVIEWED AND REFEREED INTERNATIONAL JOURNAL
(Fulfilled Suggests Parameters of UGC by IJMER)
Volume:14, Issue:8(1), August, 2025
Scopus Review ID: A2B96D3ACF3FEA2A
Article Received: Reviewed : Accepted
Publisher: Sucharitha Publication, India
Online Copy of Article Publication Available : www.ijmer.in
https://doi.org/ijmer.in/14.08(1)/2025.33

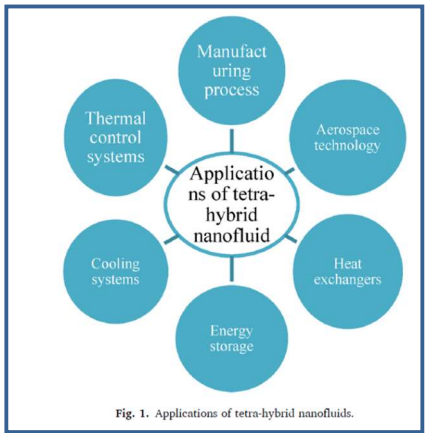


Fig.1a:. Applications of tetra-hybrid nanofluid

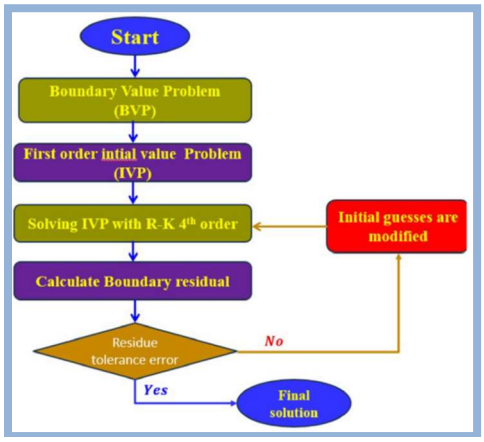


Fig.1b :Numerical procedure flow charge

1.4. Velocity, thermal and solutal slip

The no-slip boundary condition, which posits that a liquid sticks to a solid border, is commonly employed in the analysis of viscous fluid flow issues. Nonetheless, there are instances where this condition is insufficient, and slippage may transpire at the boundary when the fluid is particulate, including emulsions, suspensions, foams, and polymer solutions. The fluid flow characteristics under the slip flow regime significantly diverge from conventional flow. The slip flows under various flow configurations have been examined by Hayat et al. [37]. Velocity and temperature slips have a crucial role in the behavior of tetra-hybrid nanofluids, which are utilized in diverse applications. In contrast to traditional no-slip conditions, velocity slip permits fluid to maintain a finite velocity at the boundary, hence diminishing shear drag and improving flow, particularly in microscale systems. Temperature slip pertains to the inadequate thermal contact between the fluid and the surface, which is crucial for precise thermal modeling. The integration of slips and tetra-hybrid nanofluids results in diminished energy consumption, enhanced thermal efficiency, and superior performance in compact or high-heat settings. Multiple authors (Khan and Rasheed [38], Mingyu and Jing [39], Maranna et al. [40], Sarkar et al. [41]) have investigated the effects of slip phenomena in hydromagnetic Williamson nanofluid MoS_2–SiO_2 hybrid nanofluid flow, in conjunction with velocity slip next to an uneven three-dimensional geometry. Prasun Choudhary et al. [42] have expanded the analysis of temperature and velocity slip effects on the magnetohydrodynamic flow of tetra-hybrid nanofluids over a porous stretching surface.

1.5. Heat sources

The examination of heat generation and absorption in flowing fluids is crucial for various physical issues related to chemical processes and the dissociation of fluids. Jha and Ajibade [43] investigated the impact of heat generation and absorption on the free convective flow of viscous incompressible fluids between vertical porous plates resulting from periodic heating of the plates. They noted that heat absorption results in a reduction of both the temperature and velocity of the fluid. Jha and Ajibade [44] examined unstable free convective Couette flow of a heat-generating/absorbing fluid. Siddiqa et al. [45] examined the natural convection flow of a viscous incompressible fluid over a semi-infinite flat plate, incorporating the effects of exponentially increasing temperature-dependent viscosity and internal heat generation. Abiodun et al. [46] have examined the synergistic impact of variable viscosity and variable heat conductivity on natural convection Couette flow.

1.6. Joule heating

Dissipation effects significantly influence the efficiency of energy transmission and the thermal characteristics of nanofluids. Dissipation is employed in nanofluid heat transfer, where mechanical, thermal, and electrical forces interact intricately. Enhancing nanofluid efficacy for diverse technological and industrial applications is achievable through meticulous analysis and regulation of these impacts. Agarwal et al. [47] examined the radiative flow of magnetohydrodynamic (MHD) Powell-Eyring nanofluids over an exponentially stretched sheet, considering the effects of swimming microorganisms and viscous dissipation. Zegeyeet et al. [48] investigated the energy transport characteristics of mixed convection boundary layer flows using blood-based nanofluids, focusing on the interplay between Ohmic heating and viscous dissipation in the axisymmetric flow of Carreau nanofluids over an unstable radially extending porous disc. Panda et al. [49] investigated buoyancy-driven hybridized nanofluids in an upward permeable wedge.

Cover Page

INTERNATIONAL JOURNAL OF MULTIDISCIPLINARY EDUCATIONAL RESEARCH
ISSN:2277-7881(Print); IMPACT FACTOR :9.014(2025); IC VALUE:5.16; ISI VALUE:2.286
PEER REVIEWED AND REFEREED INTERNATIONAL JOURNAL
(Fulfilled Suggests Parameters of UGC by IJMER)
Volume:14, Issue:8(1), August, 2025
Scopus Review ID: A2B96D3ACF3FEA2A
Article Received: Reviewed : Accepted
Publisher: Sucharitha Publication, India
Online Copy of Article Publication Available : www.ijmer.in
https://doi.org/ijmer.in/14.08(1)/2025.33

Novelty

- Thorough comparative examination of tetra nanofluid (Al_2O_3 + Cu + SiO_2 + TiO_2/EG), ternary nanofluid (Al_2O_3 + Cu + SiO_2/EG), and hybrid nanofluid (Al_2O_3 + Cu/EG) under uniform thermophysical parameters.
- Concurrent integration of dual dispersion phenomena (Brownian motion and thermophoresis), thermal radiation, magnetohydrodynamic effects, and exothermic chemical reactions, which are infrequently examined together inside a singular model.
- Examination of various slip circumstances (velocity, temperature, and solutal slips) in conjunction with sophisticated multi-component nanofluids on a stretching sheet.
- Assessment of the combined effect of four nanoparticles on the augmentation of momentum, heat, and mass transfer.
- Offers a comprehensive evaluation of thermal efficiency and transport properties among hybrid, ternary, and tetra nanofluids for sophisticated engineering applications.

Research Gap

- The synergistic impacts of double dispersion, exothermic chemical reactions, heat radiation, and magnetic fields on tetra nanofluids remain little investigated.
- Scarce research has investigated numerous slip processes concurrently in thermally radiative magnetohydrodynamic convective flows of multi-hybrid nanofluids.
- Comparative examinations of hybrid, ternary, and tetra nanofluids under uniform physical circumstances are limited in the literature.
- The interplay between nanoparticle aggregation phenomena and chemical reaction kinetics in radiative magnetohydrodynamic flow systems necessitates additional examination.

Real-Time Applications

- Sophisticated cooling systems for electronic gadgets, microprocessors, and data centers necessitating substantial heat dissipation.
- Solar thermal collectors in renewable energy systems, wherein augmented thermal conductivity enhances energy conversion efficiency.
- Chemical reactors and catalytic processes that entail exothermic reactions and heat production.
- Metallurgical and polymer extrusion sectors, where sheet stretching operations are frequently utilized.
- Nuclear reactor cooling systems need effective heat dissipation and thermal equilibrium.
- Applications of biomedical engineering, encompassing targeted drug delivery and hyperthermia treatment utilizing nanoparticle-based fluids.
- Thermal management systems for automotive and aerospace applications to optimize engine and component cooling.
- Heat exchangers, refrigeration units, and energy storage systems, wherein the enhanced heat transfer capabilities of tetra nanofluids can markedly elevate operational efficiency.

This study examines the synergistic impacts of double dispersion, exothermic chemical reactions, thermal radiation, and magnetic fields on the convective heat and mass transfer of ethylene glycol-based tetra, ternary, and hybrid nanofluids containing Al_2O_3, Cu, SiO_2, and TiO_2 nanoparticles over a stretching sheet with various slip conditions. The tetra nanofluid (Al_2O_3 + Cu + SiO_2 + TiO_2/Ethylene glycol) provides superior heat and mass transfer performance compared with ternary and hybrid nanofluids, making it a promising working fluid for next-generation thermal engineering and energy systems. The governing nonlinear partial differential equations that describe momentum, energy, and concentration transport are converted into a system of ordinary differential equations by the RKF-45 numerical method and similarity transformations, and subsequently solved numerically. The effects of critical physical parameters, such as magnetic field strength, thermal radiation, velocity slip, thermal slip, solutal slip, exothermic reaction, and nanoparticle volume fraction, on the distributions of velocity (f'), temperature (θ), and nanoconcentration (Φ) are graphically analyzed for various parametric variations.

2. MATHEMATICAL MODEL AND SOLUTION:

We consider two dimensional non-linear convective tetra hybrid nanofluid flow over an expanding surface. The following assumptions are supposed in the flow problem:

Cover Page

INTERNATIONAL JOURNAL OF MULTIDISCIPLINARY EDUCATIONAL RESEARCH
ISSN:2277-7881(Print); IMPACT FACTOR :9.014(2025); IC VALUE:5.16; ISI VALUE:2.286
PEER REVIEWED AND REFEREED INTERNATIONAL JOURNAL
(Fulfilled Suggests Parameters of UGC by IJMER)
Volume:14, Issue:8(1), August, 2025
Scopus Review ID: A2B96D3ACF3FEA2A
Article Received: Reviewed : Accepted
Publisher: Sucharitha Publication, India
Online Copy of Article Publication Available : www.ijmer.in
https://doi.org/ijmer.in/14.08(1)/2025.33

(i) Four types of nanoparticles namely Al_2O_3, Cu, SiO_2 ,TiO_2 are suspended in the base fluid are taken as Ethylene Glycol to form a new composition Al_2O_3, Cu, SiO_2 ,TiO_2/Eg

(ii) To stabilize the flow and thermal properties of this new composition, the Brownian motion, thermophoresis properties, non-linear thermal radiation, and heat absorption/generation terms are incorporated into the flow field

(iii) The impact of Darcy-Forchheimer phenomenon is considered for flow model The flow occurs in the region $y \geq 0$

(iv) The flow is established due to the linear expansion of the stretching surface which appears through the slit x=y=0

(v) The expansion in the sheet is linear which is moving with linear velocity $U_m = ax$, where a is constant values and x is the non-linearity index of the stretching sheet.

(vi) Concentration and temperature of the surface are C_w, T_w while the corresponding values at the free stream are C_∞, T_∞.

(vii) Exothermic reaction with Activation energy is considered in the diffusion equation.

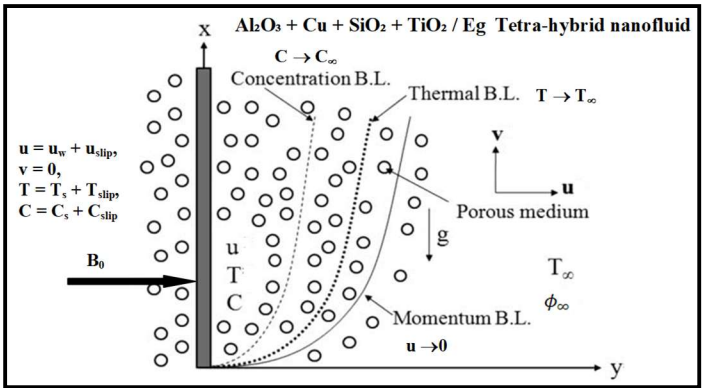


Fig. 1 : Configuration of the problem

3. GOVERNING EQUATIONS

In view of the above assumptions, the equations that governing the flow, heat and mass transfer are (Kausar et al.[50], Grubka and Bobba[51], Amudhini and De[52] and Sajide et al.[53]):

$$\frac{\partial u}{\partial x}+\frac{\partial v}{\partial y}=0 \tag{1}$$

$$\rho_{tehnf}\left(u\frac{\partial u}{\partial x}+v\frac{\partial u}{\partial y}\right)=\frac{\partial}{\partial y}\left[\mu_{tehnf}\frac{\partial u}{\partial y}\right]-\frac{\mu_{tehnf}}{k}(u)-\frac{Cb}{\sqrt{k}}(u^2)+$$
$$(\rho)_{thnf}\, g[\beta_{tehnf}(T-T_\infty)+\beta^2{}_{tehnf}(T-T_\infty)^2]+\sigma_{tehnf}(EB-B^2u) \tag{2}$$

$$(\rho C_p)_{tehnf}\left(u\frac{\partial T}{\partial x}+v\frac{\partial T}{\partial y}\right)=\frac{\partial}{\partial \bar{x}}\left(\alpha_x\frac{\partial T}{\partial \bar{x}}\right)+\frac{\partial}{\partial \bar{y}}\left(\left(\alpha_y\frac{\partial T}{\partial \bar{y}}\right)-\frac{\partial q_r}{\partial y}\right.$$
$$+Q_H(T-T_\infty)+\tau\left[D_B\left(\frac{\partial T}{\partial y}\frac{\partial C}{\partial y}\right)+\frac{D_T}{T_\infty}\left(\frac{\partial T}{\partial y}\right)^2\right]+\mu_{tehnf}\left(\frac{\partial u}{\partial y}\right)^2+\sigma_{tehnf}(T,C)\mu_e^2H_o^2(u^2)$$
$$+\mathrm{Q_1^{'}A}(C-C_\infty)(C-C_\infty)\left(\frac{T}{T_\infty}\right)^n Exp\left(-\frac{E_a}{KT}\right) \tag{3}$$

Cover Page

INTERNATIONAL JOURNAL OF MULTIDISCIPLINARY EDUCATIONAL RESEARCH
ISSN:2277-7881(Print); IMPACT FACTOR :9.014(2025); IC VALUE:5.16; ISI VALUE:2.286
PEER REVIEWED AND REFEREED INTERNATIONAL JOURNAL
(Fulfilled Suggests Parameters of UGC by IJMER)
Volume:14, Issue:8(1), August, 2025
Scopus Review ID: A2B96D3ACF3FEA2A
Article Received: Reviewed : Accepted
Publisher: Sucharitha Publication, India
Online Copy of Article Publication Available : www.ijmer.in
https://doi.org/ijmer.in/14.08(1)/2025.33

$$(u\frac{\partial C}{\partial x}+v\frac{\partial C}{\partial y})=[\frac{\partial}{\partial x}(D_x\frac{\partial C}{\partial x})+\frac{\partial}{\partial y}(D_y\frac{\partial C}{\partial y})]+(\frac{D_T}{T_\infty})\frac{\partial^2 T}{\partial y^2}$$
$$-Ak_c(C-C_\infty)(\frac{T}{T_\infty})^n Exp(-\frac{E_a}{KT}) \qquad (4)$$

where u,v depict the flow elements along x and y axes. Moreover, $(\rho C_p)_{tenf}$, ρ_{tenf}, μ_{tenf}, k_{tenf}, $(\rho\beta)_{tenf}$, σ_{tenf} are termed as heat capacitance, density, viscosity, thermal conductivity, thermal expansion and electrical conductivity for tetra hybrid nanofluiud respectively. D_B, D_T are Brownian and thermophoresis diffusions.F is non-uniform inertia coefficient,Q_H is rate of heat generation

α_x Dx and α_y, Dy are the effective thermal and solutal diffusivities respectively, have the contributions of both molecular diffusion and hydrodynamic dispersion ,these can be described as

$$\alpha_x=\alpha+\gamma d\bar{v},\alpha_y=\alpha+\gamma d\bar{u}$$
$$D_x=D+\zeta d\bar{v},D_y=D+\zeta du \qquad (5)$$

Where α is the thermal conductivity, D is the molecular diffusivities,γ is the coefficient of thermal dispersion and ζ is the solutal dispersion.

We assume that the fluid thermal conductivity α is to be varying as a linear function of temperature in the form [Seddeek and Salem[Ref:54]]

$$\alpha=\alpha_o(1+E(T-T_\infty)) \qquad (6)$$

where α_o is the thermal diffusivity at the wavy surface temperature Tw and E is a constant depending on the nature of the fluid. It is worth mentioning here that E is positive for fluids such as air and E is negative for fluids such as lubrication oils. This can be written in the non-dimensional form [Slattery[Ref:12]] as

$$\alpha=\alpha_o(1+\beta_{11}\theta) \qquad (7)$$

Where $\beta_{11}=E(T-T_\infty)$ is the thermal conductivity parameter. The variation of β_{11} can be taken in the range $-0.1\le\beta_{11}\le 0$ for lubrication oils $0\le\beta_{11}\le 0.12$ for water and $0\le\beta_{11}\le 6$ for air.

The dynamic viscosity of the nanofluids is assumed to be temperature dependent as follows:

$$\mu_f(T)=\mu_o Exp(-m(T-T_\infty)) \qquad (8)$$

where μ_o is the nanofluid viscosity at the ambient temperature T_∞ T. m is the viscosity variation parameter which depends on the particular fluid.

The non-dimensional temperature $\theta=\frac{T-T_\infty}{T_w-T_\infty}$ can be simplified as

Cover Page

INTERNATIONAL JOURNAL OF MULTIDISCIPLINARY EDUCATIONAL RESEARCH
ISSN:2277-7881(Print); IMPACT FACTOR :9.014(2025); IC VALUE:5.16; ISI VALUE:2.286
PEER REVIEWED AND REFEREED INTERNATIONAL JOURNAL
(Fulfilled Suggests Parameters of UGC by IJMER)
Volume:14, Issue:8(1), August, 2025
Scopus Review ID: A2B96D3ACF3FEA2A
Article Received: Reviewed : Accepted
Publisher: Sucharitha Publication, India
Online Copy of Article Publication Available : www.ijmer.in
https://doi.org/ijmer.in/14.08(1)/2025.33

$$T = T_\infty(1+(\theta_w-1)\theta) \tag{9}$$

where $\theta_w = \frac{T_w}{T_\infty}$ is the temperature parameter.

σ(T,C) is the variable electrical conductivity,which defined as:

$$\sigma(T,C) = \sigma_o[1+\varepsilon_1^{'}(\frac{T-T_\infty}{T_w-T_\infty})+\varepsilon_2^{'}(\frac{C-C_\infty}{C_w-C_\infty})], \tag{10}$$

Where σ_o is the constant electrical conductivity case,α_1 is the temperature dependent electrical conductivity parameter and β_1 is the nanoparticle concentration-dependent electrical conductivity parameter.

After applying the Roseland radiative heat flux,defined as $q_r = -\frac{4\sigma^{\bullet}}{3\beta_R}\frac{\partial T'^4}{\partial y}$, (11)

where $\sigma^{\bullet}\ and\ \beta_R$ are the coefficients that are used for the Stefan-Boltzmann constant and mean absorbing coefficient respectively,We propose that the variance in the temperature within the flow,containing the term T'^4 ,can be interpreted as a limear relationship of temperature .Developing T'^4 in a Taylor series abount the free stream temperature T_∞ and neglecting higher order terms,we obtain :

$$T'^4 \cong 4T_\infty^3 T - 3T_\infty^4 \tag{12}$$

Using equation(5) and Rosseland approximation(12)

equation (3&4) reduce to

$$\begin{aligned}&(\rho C_p)_{tehnf}(u\frac{\partial T}{\partial x}+v\frac{\partial T}{\partial y}) = \frac{\partial}{\partial \vec{x}}(\alpha_x\frac{\partial T}{\partial \vec{x}})+\frac{\partial}{\partial \vec{y}}((\alpha_y\frac{\partial T}{\partial \vec{y}})+(\frac{16\sigma^* T_\infty^3}{3\beta_R})\frac{\partial^2 T}{\partial y^2}-\frac{\partial q_r}{\partial y}+Q_H(T-T_\infty)\\ &+\tau[D_B(\frac{\partial T}{\partial y}\frac{\partial C}{\partial y})+\frac{D_T}{T_\infty}(\frac{\partial T}{\partial y})^2]+\mu_{tehnf}(\frac{\partial u}{\partial y})^2+\sigma_{tehnf}(T,C)\mu_e^2 H_o^2(u^2)\\ &+Q_1^{'}A(C-C_\infty)(C-C_\infty)(\frac{T}{T_\infty})^n Exp(-\frac{E_a}{KT})\end{aligned} \tag{13}$$

$$\begin{aligned}&(u\frac{\partial C}{\partial x}+v\frac{\partial C}{\partial y}) = [\frac{\partial}{\partial x}(D+\zeta d\bar{v})\frac{\partial C}{\partial x})]+\frac{\partial}{\partial y}[(D+\zeta du)\frac{\partial C}{\partial y})]+(\frac{D_T}{T_\infty})\frac{\partial^2 T}{\partial y^2}\\ &-Ak_c(C-C_\infty)(\frac{T}{T_\infty})^n Exp(-\frac{E_a}{KT})\end{aligned} \tag{14}$$

Boundary conditions:

The boundary conditions in the context of this study are listed as below(Kausar et a.[50],Grubka and Bobba[51] and Amudhini et al[52]):

Cover Page

INTERNATIONAL JOURNAL OF MULTIDISCIPLINARY EDUCATIONAL RESEARCH
ISSN:2277-7881(Print); IMPACT FACTOR :9.014(2025); IC VALUE:5.16; ISI VALUE:2.286
PEER REVIEWED AND REFEREED INTERNATIONAL JOURNAL
(Fulfilled Suggests Parameters of UGC by IJMER)
Volume:14, Issue:8(1), August, 2025
Scopus Review ID: A2B96D3ACF3FEA2A
Article Received: Reviewed : Accepted
Publisher: Sucharitha Publication, India
Online Copy of Article Publication Available : www.ijmer.in
https://doi.org/ijmer.in/14.08(1)/2025.33

$$\left.\begin{aligned} &u(x,y)=u_w+B_1'\frac{\partial u}{\partial y}=ax+B_1'\frac{\partial u}{\partial y}, v(x,y)=v_w \ \ at \ \ y=0 \\ &T=T_s+T_o x^2+B_2'\frac{\partial T}{\partial y}, C=C_s+C_o x^2+B_3'\frac{\partial C}{\partial y} \ \text{at} \ \ \ y=0 \\ &u(x,y)\to 0, v(x,y)\to 0, \mathrm{T}\to \mathrm{T}_\infty, C\to C_\infty \ \ at \ \ y\to\infty \end{aligned}\right| \qquad (15)$$

At y=0(Surface boundary)

The velocity slip condition in $u(x,y)=u_w+B_1'\frac{\partial u}{\partial y}=ax+B_1'\frac{\partial u}{\partial y}$ represents a partial slip at the surface ,whch is common in fluid flow where the no-slip condition is not valid. Here, ax indicates a stretching sheet, and the term with B_1' accounts for slip due to surface properties. Transverse velocity v=0 implies that there is no penetration of fluid ate surface and it indicates an impermeable boundary .The temperature and nanoconcentration condition includes surface temperature and concentration Ts,Cs, thermal slip Tslip, solutal slip Cslip ,quadratic spatial variation To x^2,Co x^2 and a convective term $B_2'\frac{\partial T}{\partial y}, B_3'\frac{\partial C}{\partial y}$,capturing heat and mass transfer effects near the surface, $T=T_s+T_{slip}$, $C=C_s+C_{slip}$ incorporates a non-linear thermal and solutal slip conditions and spatial variation in surface temperature and nanoconcentration.

As $y\to\infty$ (Free stream):

The conditions at $y\to\infty$ represent the free steam values for velocity($u\to 0, v\to 0$), and temperature and concentration ($\mathrm{T}\to\mathrm{T}_\infty, C\to C_\infty$)and these conditions ensure that the fluid is undisturbed far from the boundary.

The dynamic viscosity μ_{thnf} density ρ_{thnf} thermal diffusivity k_{thnf} thermal conductivity $(\rho C_P)_{thnf}$ specific heat, k_{thnf} heat capacitance, electric conductivity σ_{thnf} of the nanofluid and thermal expansion $(\rho\beta)_{thnf}$ of base fluid are defined as follows:

Table.1 Nanoparticle values

Nanofluid particles					Base fluid
Thermophysical properties	Al2o3	Cu	Sio2	Tio2	Ethylene Glycol
Density(ρ),Kg/m^3	3970	8933	2200	4250	1115
Specific heat Capacity(Cp)J/k	765	385	703	686.2	2430
Thermal conductivity(kf).W/m-k	40	401	1.2	8.8538	0.253
Thermal expansioin βx10^{-5}(K^{-1})	0.85	1.67	0.056	0.90	5.7
σ(s/m)	1.0x10^{-10}	5.96 x 10^7	1.5 x 10^{-25}	6.27x10^{-5}	10.7x10^{-5}

Table.2 Nanoparticle properties

Termophysical properties	**Tetra Hybrid Nanofluid**
Density(ρ),Kg/m^3	$(\rho)_{tehnf}=(1-\phi_4)[(1-\phi_3[(1-\phi_1)+(1-\phi_2)\rho_f+\phi_{1\rho_{s1}})+\phi_2\rho_{s2}]+\phi_4\rho_{s4}$
Viscosity(μ) N s/m^2	$\mu_{tehnf}=\frac{\mu_f}{(1-\phi_1)^{2.5}(1-\phi_2)^{2.5}(1-\phi_3)^{2.5}(1-\phi_4)^{2.5}}$
Specific heat Capacity(Cp)J/k	$(\rho C_p)_{tehnf}=(1-\phi_4)[(1-\phi_3)[(1-\phi_1)+(1-\phi_2)$ $(\rho C_p)_f+\phi_1(\rho C_p)_{s1}]+\phi_2\rho_{s2}]+\phi_4(\rho C_p)_{s4}$

Cover Page

INTERNATIONAL JOURNAL OF MULTIDISCIPLINARY EDUCATIONAL RESEARCH
ISSN:2277-7881(Print); IMPACT FACTOR :9.014(2025); IC VALUE:5.16; ISI VALUE:2.286
PEER REVIEWED AND REFEREED INTERNATIONAL JOURNAL
(Fulfilled Suggests Parameters of UGC by IJMER)
Volume:14, Issue:8(1), August, 2025
Scopus Review ID: A2B96D3ACF3FEA2A
Article Received: Reviewed : Accepted
Publisher: Sucharitha Publication, India
Online Copy of Article Publication Available : www.ijmer.in
https://doi.org/ijmer.in/14.08(1)/2025.33

Thermal conductivity(kf). W/m-k	$\frac{k_{nf}}{k_f}=\frac{k_{s1}+2k_f-2\phi_1(k_f-k_{s1})}{k_{s1}+2k_f+\phi_1(k_f-k_{s1})}$ $\frac{k_{hnf}}{k_{nf}}=\frac{k_{s2}+2k_{nf}-2\phi_2(k_{nf}-k_{s2})}{k_{s2}+2k_{nf}+\phi_2(k_{nf}-k_{s2})}$ $\frac{k_{thnf}}{k_{hnf}}=\frac{k_{s3}+2k_{hnf}-2\phi_3(k_{hnf}-k_{s3})}{k_{s3}+2k_{hnf}+\phi_3(k_{hnf}-k_{s3})}$ $\frac{k_{tehnf}}{k_{thnf}}=\frac{k_{s4}+2k_{thnf}-2\phi_4(k_{thnf}-k_{s4})}{k_{s4}+2k_{thnf}+\phi_4(k_{thnf}-k_{s4})}$
Thermal diffusivity($\beta x10^{-5}(K^{-1})$	$(\rho\beta_p)_{tehnf}=(1-\phi_4)[(1-\phi_3)[(1-\phi_1)+(1-\phi_2)$ $(\rho\beta)_f+\phi_1(\rho\beta)_{s1}]+\phi_2\rho_{s2}]+\phi_4(\rho\beta)_{s4}$
Electrical conductivity(σ(s/m))	$\frac{\sigma_{nf}}{\sigma_f}=\frac{\sigma_{s1}+2\sigma_f-2\phi_1(\sigma_f-\sigma_{s1})}{\sigma_{s1}+2\sigma_f+\phi_1(\sigma_f-\sigma_{s1}}$ $\frac{\sigma_{hnf}}{\sigma_{nf}}=\frac{\sigma_{s2}+2\sigma_{nf}-2\phi_2(\sigma_f-\sigma_{s2})}{\sigma_{s2}+2\sigma_f+\phi_2(\sigma_f-\sigma_{s2})}$ $\frac{\sigma_{thnf}}{\sigma_{hnf}}=\frac{\sigma_{s3}+2\sigma_{hnf}-2\phi_3(\sigma_f-\sigma_{s3})}{\sigma_{s3}+2\sigma_f+\phi_3(\sigma_f-\sigma}$ $\frac{\sigma_{tehnf}}{\sigma_{thnf}}=\frac{\sigma_{s4}+2\sigma_{thnf}-2\phi_4(\sigma_f-\sigma_{s4})}{\sigma_{s4}+2\sigma_f+\phi_4(\sigma_f-\sigma_{s4}}$

where the subscripts thnf, hnf, nf, *f* represent the thermo physical properties of the tri-hybrid, hybrid and mono nanofluid, base fluid respectively and ϕ is the solid volume fraction of the nanoparticles. The thermo physical properties of the nanofluid are given in Table 1.

$$A_1=[(1-\phi_1)(1-\phi_2)(1-\phi_3)(1-\phi_4)]^{2.5},\quad A_2=[(1-\phi_1)(1-\phi_{s_1}+\frac{\rho_{s1}}{\rho_f}\phi_1)+\frac{\rho_{s2}}{\rho_f}\phi_2]+\frac{\rho_{s3}}{\rho_f}\phi_3+\frac{\rho_{s4}}{\rho_f}\phi_4$$

$$A_3=[(1-\phi_1)(1-\phi_{s_1}+\frac{\beta_{s1}}{\beta_f}\phi_1)+\frac{\beta_{s2}}{\beta_f}\phi_2]+\frac{\beta_{s3}}{\beta_f}\phi_3+\frac{\beta_{s4}}{\beta_f}\phi_4$$

$$A_4=(1-\phi_3)[(1-\phi_2)(1-\phi_1+\frac{(\rho C_p)_{s1}}{(\rho C_p)_f}\phi_1)+\frac{(\rho C_p)_{s2}}{(\rho C_p)_f}\phi_2]+\frac{(\rho C_p)_{s3}}{(\rho C_p)_f}\phi_3+\frac{(\rho C_p)_{s4}}{(\rho C_p)_f}\phi_4$$

$$A_5=\frac{k_{s4}+2k_{thnf}-2\phi_3(k_{thnf}-k_{s4})}{k_{s4}+2k_{thnf}+\phi_4(k_{thnf}-k_{s4})},\ A_6=\frac{\sigma_{s4}+2\sigma_{thnf}-2\phi_4(\sigma_{thnf}-\sigma_{s4})}{\sigma_{s4}+2\sigma_{thnf}+\phi_4(\sigma_{thnf}-\sigma_{s4})}$$

Similarity transformations:

By adopting the following similarity variables(Kausar et al([50]):

Cover Page

INTERNATIONAL JOURNAL OF MULTIDISCIPLINARY EDUCATIONAL RESEARCH
ISSN:2277-7881(Print); IMPACT FACTOR :9.014(2025); IC VALUE:5.16; ISI VALUE:2.286
PEER REVIEWED AND REFEREED INTERNATIONAL JOURNAL
(Fulfilled Suggests Parameters of UGC by IJMER)
Volume:14, Issue:8(1), August, 2025
Scopus Review ID: A2B96D3ACF3FEA2A
Article Received: Reviewed : Accepted
Publisher: Sucharitha Publication, India
Online Copy of Article Publication Available : www.ijmer.in
https://doi.org/ijmer.in/14.08(1)/2025.33

$$\eta = (\sqrt{\frac{a}{\nu_f}})y, u = axf'(\eta), v = -(\sqrt{(a\nu_f)})f(\eta),\ \theta = \frac{T - T_\infty}{T_w - T_\infty}, \Phi = \frac{C - C_\infty}{C_w - C_\infty} \tag{16}$$

Using Eqns. (9) (10) , (12) and (16) the governing non-linear partial differential equations, together with the boundary conditions (15) takes the form

$$f''' - Bf'\theta' - A_1 Kf' + e^{B\theta}[A_1(ff'' - (f')^2] - (\frac{A_1 A_6}{A_2})M^2(1 + \varepsilon_1\theta + \varepsilon_2\Phi)(f') + (\frac{GA_1A_3}{A_2})(\theta + \beta_1\theta^2) - (\frac{A_1}{A_2})fs(f')^2 \tag{17}$$

$$(1 + \beta_{11}\theta + A_4 + \frac{4Rd}{3})\theta'' + \beta_{11}(\theta')^2 + \Pr(A_3)(f\theta') + Rd(\theta_w - 1)^3(3\theta^2(\theta')^2 + \theta^3\theta'') + 3Rd(\theta_w - 1)[(\theta_w - 1) + 1)](2\theta^2(\theta')^2 + \theta^2\theta'') + Q(\theta) + e^{-B\theta}Ec\Pr[(f'')^2 + (g')^2] + Ec\Pr A_6 M^2(1 + \varepsilon_1\theta + \varepsilon_2\Phi)((f')^2 + g^2) + Ds(f''\theta' + f'\theta'') = 0 \tag{18}$$

$$\Phi'' + Sc(f\Phi') - Q_1\gamma\Phi(1 + n\delta\theta)\,\mathrm{E}\,xp(-\frac{E_1}{1 + \delta\theta}) + (ScSr)\theta'' + Dc(f''\Phi' + f'\Phi'') = 0 \tag{19}$$

The transformed boundary conditions are

$$f'(0) = 1 + B_1 f''(0), \theta(0) = 1 + B_2\theta'(0)), \Phi(0) = 1 + B_3\Phi'(0)$$
$$f' \to 0, \theta \to 0, \Phi \to 0 \ \ as\ \eta \to \infty \tag{20}$$

where prime indicates ordinary differentiation with respect to η. In usual notations

where, $B = m(T_w - T_\infty)a$ (Variable viscosity parameter), $\mathrm{fs} = \frac{Cb}{\sqrt{k}}$ (Inertia parameter or Forchheimer number),

$G = \frac{\beta g(T_w - T_\infty)a^4}{\nu^2}$ (Grashof number), $Ra_d = \frac{gK\beta_T(T_w - T_\infty)a^4}{a\nu_f}$ (Pore diameter dependent Rayleigh number),

$Ds = \gamma Ra_d$, $Dc = \varsigma Ra_d$ are thermal and solutal dispersion parameters respectively, $M^2 = \frac{\sigma_o\mu_e^2 H_0^2}{a\nu_f}$ (magnetic parameter), $K = \frac{a^2}{k_p}$ (Inverse Darcy parameter), $\Pr = \frac{\mu_f C_p}{k_f}$ (Prandtl number), $Sc = \frac{\nu}{D_B}$ (Schmidt number),

$\gamma = \frac{k_c A a^2}{\mathrm{Q_1^{'}}(C_w - C_\infty)D_B}$ (Chemical Reaction parameter), $Sr = \frac{D_m K_T(T_w - T_\infty)}{T_s(C_w - C_\infty)}$ (Soret parameter), $Q_1 = \frac{Q_1^{'}\mathrm{A}(C_w - C_\infty)}{a^2(T_w - T_\infty)}$

(Frank-Kameneskii constant or Reaction rate parameter), $\theta_w = \frac{T_w}{T_\infty}, \delta = (\theta_w - 1)$ is temperature difference ratio,

Cover Page

INTERNATIONAL JOURNAL OF MULTIDISCIPLINARY EDUCATIONAL RESEARCH
ISSN:2277-7881(Print); IMPACT FACTOR :9.014(2025); IC VALUE:5.16; ISI VALUE:2.286
PEER REVIEWED AND REFEREED INTERNATIONAL JOURNAL
(Fulfilled Suggests Parameters of UGC by IJMER)
Volume:14, Issue:8(1), August, 2025
Scopus Review ID: A2B96D3ACF3FEA2A
Article Received: Reviewed : Accepted
Publisher: Sucharitha Publication, India
Online Copy of Article Publication Available : www.ijmer.in
https://doi.org/ijmer.in/14.08(1)/2025.33

$E_1 = \frac{E_a}{KT_0}$ (Activation energy parameter), $Rd = \frac{4\sigma^{\bullet}T_\infty^3}{\beta_R k_f}$ is thermal radiation, $B_1 = \frac{b}{a}$, is the velocity slip, $B_2 = B_2^{'}\sqrt{\frac{a}{\nu_f}}$ i

the thermal slip, $B_3 = B_3^{'}\sqrt{\frac{a}{\nu_f}}$ is the concentration slip, $Q = \frac{Q_H}{ax}$ is the heat source parameter,

Quantities of practical interest in this problem are the local skin-friction coefficient along *x* and *y* directions local Nusselt number. These are defined respectively as

$$C_{f_x} = \frac{f''(0)}{(1-\phi)^{2.5}\,\mathrm{Re}_x^{1/2}},\ Nu_x = -(1+Rd)\theta'(0)\,\mathrm{Re}_x^{1/2} \quad Sh_x = -\Phi'(0)\,\mathrm{Re}_x^{1/2} \tag{21}$$

The transformed boundary conditions are

$$f'(0) = 1 + B_1 f''(0), \theta(0) = 1 + B_2\theta'(0)), \Phi(0) = 1 + B_3\Phi'(0)$$
$$f' \to 0, \theta \to 0, \Phi \to 0 \ \ as\ \eta \to \infty \tag{22}$$

where prime indicates ordinary differentiation with respect to η.

4. PHYSICAL QUATITIES OF ENGINEERING INTERESTS

In view of the engineering and practical applications, the exploration of some physical quantities i.e the skin friction(Cf) and local rate of heat and mass transfer (Nux, Shx)have enormous significance. These physical quantities are defined as

$$C_{f_x} = \frac{f''(0)}{(1-\phi)^{2.5}\,\mathrm{Re}_x^{1/2}},\ Nu_x = -(1+Rd\theta_w)^2\theta'(0)\,\mathrm{Re}_x^{1/2} \quad Sh_x = -\Phi'(0)\,\mathrm{Re}_x^{1/2} \tag{23}$$

5. IMPLITATION OF NUMERICAL METHOD:

Due to complexity and highly non-linearity of the mathematical model represented by equations (11)-(14) along with the boundary conditions (9), it is possible to solve those with the aid of analytical techniques. Therefore, we solved the system of equations by employing shooting technique with the help of Runge-Kutta-Fehlberg method (RKF45). In this technique, at first the equations (11)-(14) are converted into five first order differential equations. After that, RKF method is executed to solve these sets of the differential equations. The detailed explanation of Shooting technique and RKF method are given below:

5.1. Shooting method:

The shooting method is technique for obtain the solution of boundary value problem(BVP).In this technique,we are converting the given higher order boundary value problem into a system of first order initial value problem(IVP).In this technique we choose the random value of one of the initial value problem and try to get the solution at other end with the help of Runge-Kutta-Fehlberg method(RKF45)by taking suitable step size h.If we are getting the solution at the other end which is equal to given boundary value problem then our guess is correct otherwise, again make the guess with te help of Secant method and repeat the same process until we are getting the desired solution at the other end.

5.2 Runge-Kutta-Fehlberg method(RKF45):

One way to guarantee accuracy in the solution of an IVP is to solve the problem twice using step size h and h/2 and compare answers at the mesh points corresponding to the larger step size. But this requires a significant amount of computation for the smaller step size and must be repeated if it is determined that the agreement is not good enough.

The Runge-Kutta-Fehlberg method (RKF45) is one way to try to resolve this problem. It has a procedure to determine if the proper step size h is being used. At each step, two different approximations for two answers do not agree to a specified accuracy, the step size is reduced. If the answers agree to more digits than required, the step size is increased.

Each step requires the use of the following six values:

Cover Page

INTERNATIONAL JOURNAL OF MULTIDISCIPLINARY EDUCATIONAL RESEARCH
ISSN:2277-7881(Print); IMPACT FACTOR :9.014(2025); IC VALUE:5.16; ISI VALUE:2.286
PEER REVIEWED AND REFEREED INTERNATIONAL JOURNAL
(Fulfilled Suggests Parameters of UGC by IJMER)
Volume:14, Issue:8(1), August, 2025
Scopus Review ID: A2B96D3ACF3FEA2A
Article Received: Reviewed : Accepted
Publisher: Sucharitha Publication, India
Online Copy of Article Publication Available : www.ijmer.in
https://doi.org/ijmer.in/14.08(1)/2025.33

$$k_1 = hf(t_k, y_k),\ k_2 = hf(t_k + \frac{h}{4}, y_k + \frac{k_1}{4})$$

$$k_3 = hf(t_k + \frac{3h}{8}, y_k + \frac{3k_1}{32} + \frac{9k_2}{32})$$

$$k_4 = hf(t_k + \frac{12h}{13}, y_k + \frac{1932k_1}{2187} + \frac{7200k_2}{2197} + \frac{7296k_3}{2197})$$

$$k_5 = hf(t_k + \frac{12h}{13}, y_k + \frac{439k_1}{216} - 8k_2 + \frac{3680k_3}{513} - \frac{845k_4}{4105})$$

$$k_6 = hf(t_k + \frac{h}{2}, y_k - \frac{8k_1}{27} + 2k_2 - \frac{3544k_3}{2565} + \frac{1849k_4}{4104} - \frac{13k_5}{49}) \quad (24)$$

The an approximation to the solution of the IVP is made using a Runge-Kutta-Fehlberg method of order 4:

$$y_{k+1} = y_k + \frac{25}{216}k_1 + \frac{1408k_3}{2565} + \frac{2197k_4}{4101} - \frac{k_5}{5}) \quad (25)$$

Where the four function values f1. f3. f4 and f5 are used. Notice that f2 is not used in the formula (22).A better value for the solution is determined using a Runge-Kutta method of order 5:

$$z_{k+1} = y_k + \frac{16}{135}k_1 + \frac{6656k_3}{12825} + \frac{28561k_4}{56430} - \frac{9k_5}{50} + \frac{2k_6}{55}) \quad (26)$$

The optimal step size (s) can be determined by multiplying the scalar s times the current step size h. The scalar s is

$$s = (\frac{tol(h)}{2[z_{k+1} - y_{k+1}]})^{1/4} \approx 0.84(\frac{tol(h)}{2[z_{k+1} - y_{k+1}]})^{1/4} \quad (27)$$

Where *tol* is the specified error control tolerance.

The derivation of the formula 24 can be found in advanced books on numerical analysis. It is important to learn that a fixed step size is not the best strategy even though it would give a nicer-appearing table of values. If values are needed that are not in the table, polynomial interpretation should be used.

6. COMPARISON

Table.3 Numerical comparison of Nu(0) for different values of Pr on stretching sheet when K=B1=B2=M=Rd=Q=Ec=0 and $\phi_1=\phi_2=\phi_3=\phi_4=0$

Pr	Nu(0)			
	Kausar et al[50]	**Grubka and Bobba[51]**	**Prasun Choudhary et al[42]**	**Present values**
0.72	1.09006	1.0885	1.087788	**1.088982**
10	1.33333	1.3333	1.333328	**1.333330**
30	2.50955	2.5097	2.509705	**2.509701**
100	4.79677	4.7969	4.796690	**4.796690**
1000	15.7118	15.7120	15.71153	**15.71192**

Table.4 : Values of Skin friction(τ(0) in Tetra-hybrid nanofluids(Al2o3-Cu-Sio2) with Ds=Dc=0,B1=0.5, B2=0.2

$$\phi_3 = \phi_2 = \phi_1 = \phi_4 = 0.02$$

Parameters		Prasun Choudhary et al[42]			**Present outcomes**		
M	K	Hybrid nanofluid	Ternary nanofluid	Tetra nanofluid	**Hybrid nanofluid**	**Ternary nanofluid**	**Tetra nanofluid**
0.1	0.2	-1.0179	-1.18424	-1.39805	**-1.0180**	**-1.18429**	**-1.39801**

Cover Page

INTERNATIONAL JOURNAL OF MULTIDISCIPLINARY EDUCATIONAL RESEARCH
ISSN:2277-7881(Print); IMPACT FACTOR :9.014(2025); IC VALUE:5.16; ISI VALUE:2.286
PEER REVIEWED AND REFEREED INTERNATIONAL JOURNAL
(Fulfilled Suggests Parameters of UGC by IJMER)
Volume:14, Issue:8(1), August, 2025
Scopus Review ID: A2B96D3ACF3FEA2A
Article Received: Reviewed : Accepted
Publisher: Sucharitha Publication, India
Online Copy of Article Publication Available : www.ijmer.in
https://doi.org/ijmer.in/14.08(1)/2025.33

0.2	0.2	-1.0288	-1.20009	-1.42061	**-1.0287**	**-1.20007**	**-1.42064**
0.3	0.2	-1.0344	-1.21018	-1.43121	**-1.0349**	**-1.21016**	**-1.43126**
0.1	0.4	-1.0189	-1.19499	-1.40842	**-1.0890**	**-1.19493**	**-1.40847**
0.1	0.6	-1.0216	-1.22544	-1.42402	**-1.0219**	**-1.22541**	**-1.42400**

Table.5 : Values of Nusselt number(Nu(0)) in Tetra-hybrid nanofluid (Al2o3+Cu+Sio2+Tio2) with Ds=Dc=0,B1=0.5, B2=0.2, $\phi_3 = \phi_2 = \phi_1 = \phi_4 = 0.02$

Parameters					Prasun Choudhary et al[42]			**Present outcomes**		
M	K	Rd	Ec	Q	Hybrid nanofluid	Ternary nanofluid	Tetra nanofluid	**Hybrid nanofluid**	**Ternary nanofluid**	**Tetra nanofluid**
0.1	0.2	0.5	0.1	0.2	2.07529	1.98934	1.94221	**2.07531**	**1.98931**	**1.94221**
0.2					2.02781	1.93297	1.86725	**2.02786**	**1.93306**	**1.86722**
0.3	0.2				2.00984	1.91189	1.85679	**2.00987**	**1.91189**	**1.85679**
	0.4				2.06413	2.09433	2.05576	**2.06411**	**2.09432**	**2.05574**
	0.6	0.5			1.63774	1.96893	1.90051	**1.63772**	**1.96899**	**1.90056**
		1.5			2.10131	1.54779	1.84432	**2.10126**	**1.54782**	**1.84437**
		3.5	0.1		2,08254	1.53946	1.83246	**2,08254**	**1.53946**	**1.83247**
			0.2		2.08554	1.98216	1.93971	**2.08552**	**1.98211**	**1.93971**
			0.3	0.2	1.78745	2.00048	1.50942	**1.78741**	**2.00056**	**1.50948**
				0.4	2.21577	2.11737	1.92489	**2.21583**	**2.11736**	**1.92480**
				0.6	2.22046	2.12468	1.91504	**2.22051**	**2.12461**	**1.91503**

7. SKIN FRICTION, NUSSELT NUMBER and SHERWOOD NUMBER

The physical quantities of engineering interest in this problem are the skin friction coefficient Cf, the Local Nusselt number Nux , the Local Sherwood number Shx which are expressed as

$$cf_x = \frac{\mu_{thnf}}{\mu_f a x^2}\left(\frac{\partial u}{\partial y}\right)_{y=0}, \quad Nu_x = -\frac{k_{thnf}}{k_f(T_w - T_\infty)}\left(\frac{\partial T}{\partial y}\right)_{y=0}, \quad Sh_x = -D_B\left(\frac{\partial C}{\partial y}\right)_{y=0}$$

8. RESULTS AND DISCUSSION:

The non-dimensional linear velocity f'(η), temperature θ(η) and nanoparticle volume fraction Φ(η) for various values of different parameters are exhibited in figs.2-30 in Eg-based tetra Hybrid nanofluids.

In this section, a graphical interpretation of the influence of various flow parameters on velocity, temperature and nanoconcentration distributions with their physical significance. The variation of skin friction, rate of heat and mass transfer are also examined through graphical representation s and tabular data. Fixed values of parameters in the computational analysis process are taken as : ϕ1=ϕ2=ϕ3=ϕ4=0.03, G=2,K=0.2, M=0.3, fs=0.1, Rd=.0.5, Ec=0.1, Q=0.5, B1=0.1, B2=0.2,B3=0.2,Ds=0.1,Dc=0.2, Pr=6.2, Sc=0.24, γ=0.5, Sr=0.5, Q1=0.5, E1=0.1, δ=0.2, n=0.2.

To ensure the numerical accuracy ,the values of $f''(0)$ and $f(\infty)$ by present method are compared with the results of Magyari and Keller[55] and Bhattacharya and Layek[56] in Table.1 without magnetic field (M=0), non-porous media (K=0, fs=0) and having no rotational motion (R=0) and with non-porous stretching sheet (fw=0), no velocity, thermal and solutal slips (B1=0=B2=B3) and those are found to be in excellent agreement. Thus, we are very much confident that the present results are accurate.

From Figs.2a-c, increasing Nanoparticle Volume Fraction (ϕ) enhances the velocity(f'), temperature(θ), and concentration(Φ) distributions. As the nanoparticle volume fraction increases, more solid nanoparticles are suspended in the base fluid. These particles possess much higher thermal conductivity than ethylene glycol, creating additional heat-conduction pathways. Consequently, heat transfer from the surface to the fluid becomes more efficient, increasing the temperature field. The enhanced thermal energy strengthens buoyancy forces, which accelerate the fluid and increase the velocity profile. The presence of more nanoparticles also raises the nanoparticle concentration distribution within the boundary layer. The tetra nanofluid exhibits the highest thermal and concentration profiles, followed by ternary and hybrid nanofluids, due to improved thermal conductivity and heat transport.

Cover Page

INTERNATIONAL JOURNAL OF MULTIDISCIPLINARY EDUCATIONAL RESEARCH
ISSN:2277-7881(Print); IMPACT FACTOR :9.014(2025); IC VALUE:5.16; ISI VALUE:2.286
PEER REVIEWED AND REFEREED INTERNATIONAL JOURNAL
(Fulfilled Suggests Parameters of UGC by IJMER)
Volume:14, Issue:8(1), August, 2025
Scopus Review ID: A2B96D3ACF3FEA2A
Article Received: Reviewed : Accepted
Publisher: Sucharitha Publication, India
Online Copy of Article Publication Available : www.ijmer.in
https://doi.org/ijmer.in/14.08(1)/2025.33

From Figs.3a-c, higher Grashof number(G) significantly increases the f'because of stronger buoyancy forces. θ & Φ boundary layers become thinner as G increases. The stronger buoyancy force accelerates the fluid motion, leading to higher velocity. As convection becomes dominant, heat and mass are transported more rapidly away from the surface, modifying the temperature and concentration boundary layers. Tetra nanofluid consistently shows superior enhancement compared to ternary and hybrid nanofluids.

From Figs.4a-c, increasing magnetic parameter(M) suppresses fluid f' due to the Lorentz force. θ & Φ increase because the magnetic field retards the flow and converts kinetic energy into thermal energy. This electromagnetic braking force suppresses velocity. The reduced fluid motion causes heat to remain longer within the boundary layer, resulting in higher temperatures. Similarly, nanoparticle diffusion slows down, causing an increase in concentration levels near the surface.

From Figs.5a-c, Larger values of Inverse Darcy Parameter (K) increase resistance offered by the porous medium, reducing f'. θ & Φ profiles rise owing to enhanced fluid retention within the porous structure. This resistance slows the fluid velocity. Due to reduced convection, thermal energy accumulates within the fluid, causing temperature enhancement. Nanoparticles also remain longer in the boundary layer, increasing concentration levels.

From Figs.6a-c, increasing Forchheimer Parameter (fs) decreases f'. θ & Φ boundary layers become thicker, leading to higher temperature and concentration distributions. The slower motion decreases the rate of heat and mass transport away from the surface, causing thicker thermal and concentration boundary layers and consequently higher temperature and concentration profiles.

From Figs.7a-c, Thermal radiation(Rd) considerably elevates temperature profiles. f' & Φ also increase because additional radiative heat energy enhances fluid motion and diffusion. Thermal radiation acts as an additional mode of heat transfer. Increasing Rd injects more thermal energy into the fluid, which elevates the temperature profile throughout the boundary layer. The increased temperature difference strengthens buoyancy forces, promoting fluid motion and enhancing velocity. The higher thermal energy also facilitates nanoparticle diffusion, increasing concentration distribution.

From Figs.8a-c, Higher Eckert number(Ec) increases θ due to viscous dissipation effects. Velocity and concentration profiles are also enhanced as mechanical energy is transformed into thermal energy within the fluid. The resulting increase in buoyancy enhances velocity, while the elevated thermal energy promotes nanoparticle movement and concentration distribution.

From Figs.9a-c, an increase in the heat source parameter (Q) enhances the thermal energy within the boundary layer, leading to a rise in temperature (θ) and concentration (Φ) profiles, while the velocity profile (f') shows a slight enhancement. This extra energy raises the fluid temperature and strengthens thermal buoyancy forces, which accelerate the fluid motion. The elevated temperature also enhances nanoparticle diffusion, leading to higher concentration profiles. Consequently, velocity, temperature, and concentration distributions increase with increasing Q.

From figs.10a-c, The velocity slip parameter(B1) allows partial fluid slip at the wall instead of the conventional no-slip condition. Increasing B1B_1B1 reduces wall friction and shear stress, enabling the fluid to move more freely near the surface. Consequently, velocity increases. However, reduced wall-fluid interaction weakens heat and mass transfer from the surface, causing slight reductions in temperature and concentration fields.

From figs.11a-c, thermal slip parameter (B2) reduces the direct transfer of heat from the wall to the fluid. As B2 increases, the fluid receives less thermal energy from the heated surface, causing the temperature profile to decrease. The reduced thermal energy weakens buoyancy forces and diminishes nanoparticle diffusion, resulting in lower velocity and concentration distributions.

From figs.12a-c, an increase in solutal slip parameter (B3) weakens species diffusion from the wall, resulting in a reduction of concentration (Φ). f' and temperature distributions are only marginally affected. The tetra nanofluid consistently demonstrates superior transport characteristics.

The thermal dispersion parameter (Ds) is shown in Figs. 13a-13c for f', θ & Φ, and Fig. 13(a) shows how thermal dispersion parameter (Ds) affects velocity distribution. Increasing Ds improves boundary layer velocity profile. Thermal dispersion increases nanofluid thermal transport, lowering viscous resistance and boosting fluid motion. The tetra nanofluid (Al_2O_3 + Cu + SiO_2 + TiO_2/Eg) has the highest velocity compared to ternary and hybrid nanofluids due to its exceptional thermal conductivity and energy transport. As Ds grows, momentum boundary layer thickness increases. Thermal dispersion parameter increases greatly raise the temperature profile, as seen in Figure 13(b). Thermal dispersion increases boundary layer fluid temperature by diffusing thermal energy from hotter to cooler locations. Tetra nanofluid has the highest temperature distribution, followed by ternary and hybrid. This is due to numerous nanoparticles' cumulative thermal conductivity improvement. As thermal dispersion parameter increases, Fig. 13(c) concentration distribution increases. Thermal dispersion improves molecular diffusion and fluid species transport. Thus, the concentration boundary layer thickens. Tetra nanofluids have larger concentrations than ternary and hybrid nanofluids because to better particle interaction and transport. Tetra nanofluids outperform ternary and hybrid nanofluids in velocity, temperature, and concentration. This shows that adding nanoparticles to ethylene glycol-based nanofluids increases heat and mass transmission.

Figs.14a-14c represent f',θ and Φ with solutal dispersion parameter(Dc). Figure 14(a) depicts the effect of the solutal dispersion parameter (Dc) on velocity. An increase in Dc leads to an enhancement in the velocity profile. Higher solutal dispersion promotes

Cover Page

INTERNATIONAL JOURNAL OF MULTIDISCIPLINARY EDUCATIONAL RESEARCH
ISSN:2277-7881(Print); IMPACT FACTOR :9.014(2025); IC VALUE:5.16; ISI VALUE:2.286
PEER REVIEWED AND REFEREED INTERNATIONAL JOURNAL
(Fulfilled Suggests Parameters of UGC by IJMER)
Volume:14, Issue:8(1), August, 2025
Scopus Review ID: A2B96D3ACF3FEA2A
Article Received: Reviewed : Accepted
Publisher: Sucharitha Publication, India
Online Copy of Article Publication Available : www.ijmer.in
https://doi.org/ijmer.in/14.08(1)/2025.33

species transport and reduces concentration gradients, which subsequently weakens the resistive forces acting on the fluid. As a result, fluid motion is accelerated. The tetra nanofluid exhibits the maximum velocity enhancement among all nanofluids considered. The temperature profile increases with increasing Dc, as illustrated in Fig. 14(b). Enhanced solutal dispersion improves the interaction between heat and mass transfer mechanisms, thereby facilitating thermal energy transport within the fluid. The temperature boundary layer thickness therefore increases with Dc. The tetra nanofluid again records the highest thermal performance due to its improved thermophysical properties. Figure 14(c) reveals that concentration profiles increase considerably with increasing Dc. Physically, a larger solutal dispersion parameter intensifies species diffusion and enhances mass transport. Consequently, concentration gradients become smoother and concentration boundary layer thickness increases. The tetra nanofluid displays the highest concentration profile, followed by ternary and hybrid nanofluids. The solutal dispersion parameter significantly enhances velocity, temperature, and concentration distributions. The tetra nanofluid demonstrates the most pronounced enhancement owing to the synergistic effects of Al_2O_3, Cu, SiO_2, and TiO_2 nanoparticles dispersed in ethylene glycol. These results confirm that tetra nanofluids possess superior heat and mass transfer capabilities compared with ternary and hybrid nanofluids.

From fig.15, higher Prandtl number(Pr) values reduce thermal diffusivity, causing a decrease in temperature distribution and thermal boundary layer thickness. Consequently, heat transfer at the surface is enhanced. As a result, heat diffuses less effectively from the heated surface, causing the thermal boundary layer to become thinner and reducing the temperature profile. The reduction in thermal energy weakens buoyancy effects, leading to lower velocity and concentration distributions. The tetra-hybrid nanofluid still exhibits the highest thermal performance compared with ternary and hybrid nanofluids.

From figs.16a-c, higher Schmidt number (Sc) values correspond to lower mass diffusivity, causing a significant reduction in concentration profiles and concentration boundary layer thickness. f' and θ distributions remain almost unchanged.

From figs.17a-c, Increasing the chemical reaction parameter(γ) intensifies the consumption of nanoparticles through reactive processes. This reduces the concentration distribution within the fluid. The decrease in concentration weakens concentration-driven buoyancy forces, leading to lower velocity and temperature profiles. Stronger reactions therefore suppress mass transport in the boundary layer.

From figs.18 a-c, The Soret effect(Sr) (thermal diffusion) causes nanoparticles to migrate from hot regions to cooler regions due to temperature gradients. As Sr increases, this thermally induced mass transfer becomes stronger, increasing nanoparticle concentration. The enhanced concentration field contributes to buoyancy effects, which in turn elevate velocity and temperature profiles.

From figs.19a-c, An increase in reaction rate accelerates species consumption within the fluid. Faster chemical reactions reduce nanoparticle concentration and weaken concentration-induced buoyancy forces. Consequently, velocity, temperature, and concentration distributions generally decrease as Q1 increases.

From figs.20 a-c, Activation energy(E1) represents the minimum energy required for a chemical reaction to occur. Higher activation energy suppresses the reaction rate because fewer molecules possess sufficient energy to react. This reduction in reaction activity preserves more nanoparticles within the fluid, increasing concentration. The enhanced concentration promotes buoyancy effects, leading to increases in velocity and temperature profiles.

From figs.21 a-c, higher values of the temperature difference ratio (δ) enhance thermal transport, leading to an increase in temperature and concentration profiles. The thermal boundary layer becomes thicker, indicating stronger heat transfer effects.

From figs.22a-c, an increase in the power-law index (n) strengthens the velocity distribution and momentum boundary layer thickness. The temperature and concentration fields also increase due to enhanced fluid motion and improved thermal transport.

We now discuss the variations of the physical quantities of engineering importance, that is ,the local skin friction coefficient for linear velocity, Cf, the local Nusselt number Nux, local Sherwood number for different values of G,M,K,fs,B1,B2,B3,Q,Rd,Ec,Ds,Dc,Pr,Sc,γ,Sr,Q1,E1,δ,n. The quantities $f''(0)$, (0),$\theta'(0)$ and $\Phi'(0)$ related to local skin friction coefficient for linear velocity(τx), the local Nusselt Number(Nu), local Sherwood number(Sh) are shown in figs.23-30 for various values of parameters.

From figs.23-25, it is observed that the skin friction component(τx(0)) grows with increase in Grashof number(G)/magnetic parameter(M)/inverse Darcy parameter(K)/Forchheimer parameter(fs)/ Temperature dependent heat sources(Q)/Thermal Radiation parameter(Rd)/Eckert number(Ec/nanoparticle volume fraction (ϕ) at the wall(η=0)in Eg based Tetra /Ternary/Hybrid nanofluids.It upsurges at the wall with enhancement in thermal dispersion parameter (Ds), in Eg based tetra/ternary/hybrid nanofluids. From the above analysis it is noticed that the values of skin friction(τ) at η=0 in Eg based Tetra nanofluid are smaller than those in Eg based ternary/hybrid nanofluid for parametric variations in G/M/K/fs/Rd/Ec/B/Q/B1/ B2/ϕ/Ds.

The rate of heat transfer (Nusselt number)(Nu) at the wall(η=0) with various parameters is demonstrated in figs.26-28 for different parameters. From the figures it is shown that it decays with rise in thermal radiation parameter(Rd)/Eckert number(Ec)/Heat generating source(Q)/thermal slip(B2)/Prandtl number(Pr)/ solutal dispersion parameter (Dc)/nanoparticle volume fraction(ϕ). Higher

Cover Page

INTERNATIONAL JOURNAL OF MULTIDISCIPLINARY EDUCATIONAL RESEARCH
ISSN:2277-7881(Print); IMPACT FACTOR :9.014(2025); IC VALUE:5.16; ISI VALUE:2.286
PEER REVIEWED AND REFEREED INTERNATIONAL JOURNAL
(Fulfilled Suggests Parameters of UGC by IJMER)
Volume:14, Issue:8(1), August, 2025
Scopus Review ID: A2B96D3ACF3FEA2A
Article Received: Reviewed : Accepted
Publisher: Sucharitha Publication, India
Online Copy of Article Publication Available : www.ijmer.in
https://doi.org/ijmer.in/14.08(1)/2025.33

the thermo-diffusion effect(Sr)/ Radiation absorption (Q1)reduces Nu at η=0 in Eg based Tetra/ternary/hybrid nanofluids. The rate of heat transfer(Nu) experiences augmentation with rise in Activation energy parameter(E1) /temperature difference ratio(δ)upsurges Nu at the wall in all types of types of nanofluids. From the above analysis it is noticed that the values of Nusselt number(Nu) in Eg based tetra nanofluid are relatively lesser than those in Eg based ternary/hybrid nanofluids for variation in Rd/Ec/Q/Dc/B2/Pr/ϕ/Q1/E1/δ.

The rate of mass transfer(Sherwood number)(Sh) at the wall(η=0)with various parameters is shown in figd.29 & 30 for different parameters. From the profiles it is found that the rate of mass transfer(Sh) lesser the molecular diffusivity(Sc)/Chemical reaction parameter(γ)/higher the thermo-diffusion effects(Sr) enhances at the wall. Increase in concentration slip(B3)/ solutal dispersion parameter (Dc) grows Sh at η=0(fig.37). Higher the radiation absorption(Q1)/nanoparticle volume fraction(ϕ)/Activation energy(E1)/ temperature difference ratio(δ) larger the Sherwood number at the wall(η=0).From the above analysis it is found that the rate of mass transfer(Sh)at the wall in Eg based tetra nanofluid are relatively greater than those in Eg based ternary/hybrid nanofluid with variation in Sc/γ/Sr/Q1/B3/ϕ/Dc/E1/δ.

9. CONCLUSION:

The effect of non-linear thermal radiation, velocity, thermal, concentration slips, activation energy ,variable viscosity and thermal conductivity on non-Darcy MHD convective heat transfer flow of Tetra hybrid nanofluid past a linear stretching sheet is considered. The equations governing the flow have been executed by numerical method. The conclusions of this analysis are:

1. Increase in Grasshof number(G)reduces the axial f', θ and Φ in Ethylene based tetra/ternary/hybrid nanofluids. τ decays, Nu ,Sh grows with increase in G at η=0 in all types of nanofluids.
2. Increase Magnetic parameter(M)/Inverse Darcy parameter(K) reduces (f') and enhances θ,Φ. τ grows, Nu, Sh decays with increase in M/K at η=0 in Eg based tetra/ternary /hybrid nanofluids.
3. Higher radiative heat flux(Rd)/Dissipative energy(Ec) larger f', θ in Eg based tetra/ternary/hybrid nanofluids. Φ enhances with rise in Rd and decays with β11 in all nanofluids.τ,Nu decays with rise in Rd/Ec. Sh grows with increase in Rd/Ec at η=0 in Eg based tetra/ternary/hybrid nanofluids.
5. f',θ and Φ enhance with higher activation energy(E1) in Eg based tetra/ternary/hybrid nanofluids. f' increases, θ and Φ deceases with rise in temperature difference ratio(δ). τ decays at η=0 with rise in E1 & δ. Nu, Sh decay with rise in E1 and grows with rise in δ at the wall in all types of nanofluids.
6. f',θ and Φ decay with first order velocity slip(B1)/thermal slip(B2)/concentration slip(B3) in E basee tetra/ternary/hybrid nanofluids.τ,Nu and Sh reduce with increase in B1/B2/B3 at η=0 in Eg based tetra/ternary/hybrid nanofluids..
7. Increase in nanoparticle volume fraction(ϕ) upsurges f',θ and Φ in Eg based Tetra/ternary/hybrud nanofluids. τ decays, Nu and Sh experience enhancement with increase in ϕ at η==0 in Eg based tetra/ternary/hybrid nanofluids.
8. Velocity enhances with rise in chemical reaction(γ)/Soret parameter(Sr) and reduces with radiation(Q1).θ enhances with γ and enhances with Sr/Q1 in all types of nanofluids.Φ reduces with rise in γ/Sr and grows with Q1.τ,Nu decay with rise in γ/Sr and grows with Q1 at η=0.Shreduces with increase in Q1/Sr and decreases with γ in all types of nanofluids.
9. Increasing thermal dispersion (Ds) enhances momentum, thermal, and concentration boundary layers.
10. Increasing solutal dispersion (Dc) significantly improves heat and mass transfer characteristics.

Among all nanofluids studied, the tetra nanofluid (Al_2O_3 + Cu + SiO_2 + TiO_2 / EG) consistently produces the highest velocity, temperature, and nanoparticle concentration profiles, indicating superior heat transfer performance compared with the ternary and hybrid nanofluids. For all graphical comparisons, the Al_2O_3 + Cu + SiO_2 + TiO_2 / Ethylene Glycol tetra-hybrid nanofluid exhibits superior thermal and mass transport characteristics compared with the ternary (Al_2O_3 + Cu + SiO_2/Eg) and hybrid (Al_2O_3 + Cu/Eg) nanofluids, owing to the combined effect of multiple nanoparticles and enhanced effective thermal conductivity.

Cover Page

INTERNATIONAL JOURNAL OF MULTIDISCIPLINARY EDUCATIONAL RESEARCH
ISSN:2277-7881(Print); IMPACT FACTOR :9.014(2025); IC VALUE:5.16; ISI VALUE:2.286
PEER REVIEWED AND REFEREED INTERNATIONAL JOURNAL
(Fulfilled Suggests Parameters of UGC by IJMER)
Volume:14, Issue:8(1), August, 2025
Scopus Review ID: A2B96D3ACF3FEA2A
Article Received: Reviewed : Accepted
Publisher: Sucharitha Publication, India
Online Copy of Article Publication Available : www.ijmer.in
https://doi.org/ijmer.in/14.08(1)/2025.33

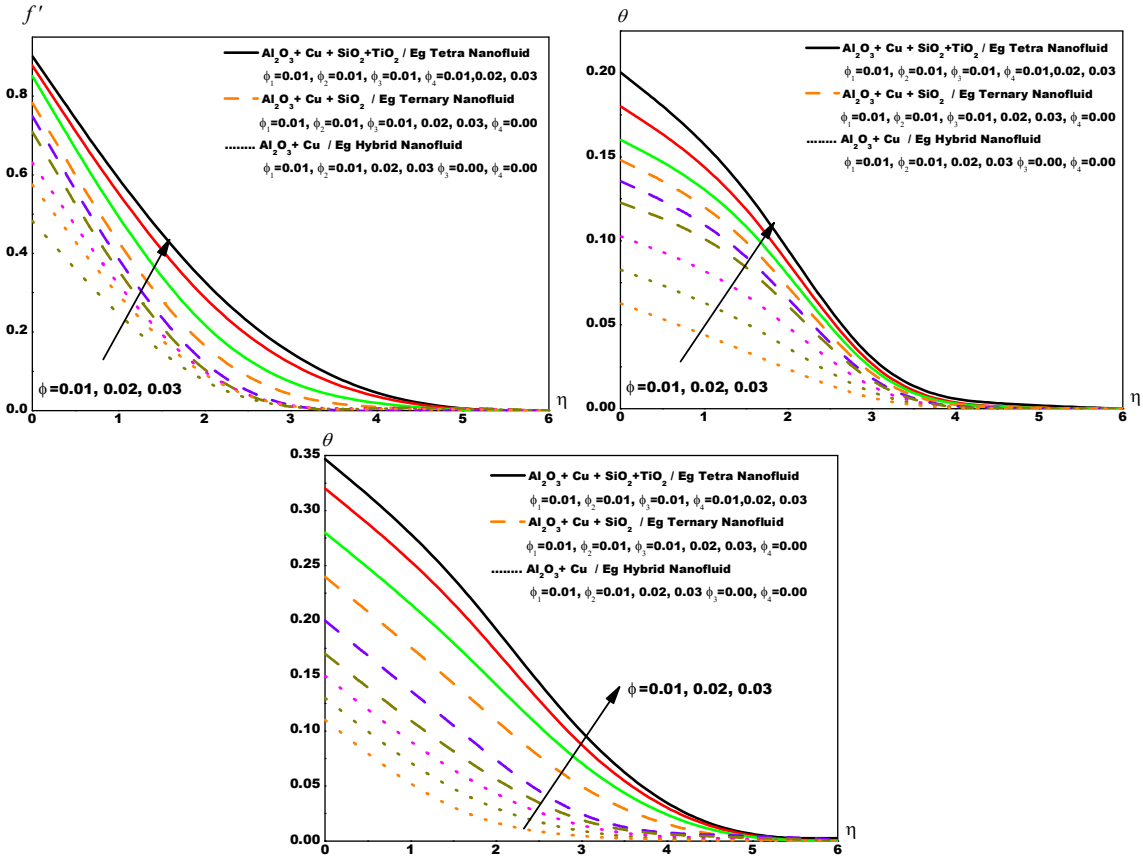


Fig.2 : Variation of [a] Velocity (f'), [b], Temperature(θ), Nanoconcentration(Φ) with Nanoparticle value fraction(ϕ)
G=2,K=0.2, M=0.3, fs=0.1, Rd=.0.5, Ec=0.1, Q=0.5, B1=0.1, B2=0.2,B3=0.2,Ds=0.1,Dc=0.2, Pr=6.2, Sc=0.24, γ=0.5, Sr=0.5, Q1=0.5, E1=0.1, δ=0.2, n=0.2

Cover Page

INTERNATIONAL JOURNAL OF MULTIDISCIPLINARY EDUCATIONAL RESEARCH
ISSN:2277-7881(Print); IMPACT FACTOR :9.014(2025); IC VALUE:5.16; ISI VALUE:2.286
PEER REVIEWED AND REFEREED INTERNATIONAL JOURNAL
(Fulfilled Suggests Parameters of UGC by IJMER)
Volume:14, Issue:8(1), August, 2025
Scopus Review ID: A2B96D3ACF3FEA2A
Article Received: Reviewed : Accepted
Publisher: Sucharitha Publication, India
Online Copy of Article Publication Available : www.ijmer.in
https://doi.org/ijmer.in/14.08(1)/2025.33

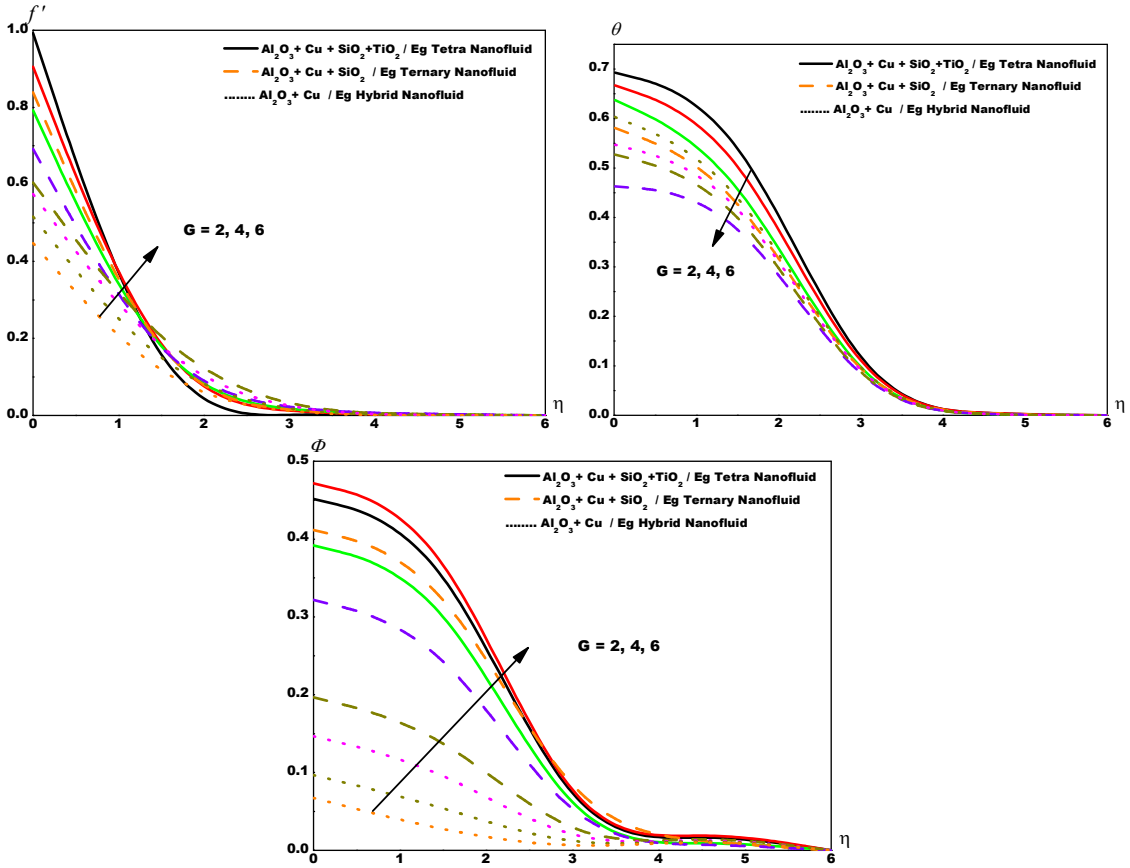


Fig.3 : Impact on Grashof of [a] f', [b] θ, [c] Φ

Cover Page

INTERNATIONAL JOURNAL OF MULTIDISCIPLINARY EDUCATIONAL RESEARCH
ISSN:2277-7881(Print); IMPACT FACTOR :9.014(2025); IC VALUE:5.16; ISI VALUE:2.286
PEER REVIEWED AND REFEREED INTERNATIONAL JOURNAL
(Fulfilled Suggests Parameters of UGC by IJMER)
Volume:14, Issue:8(1), August, 2025
Scopus Review ID: A2B96D3ACF3FEA2A
Article Received: Reviewed : Accepted
Publisher: Sucharitha Publication, India
Online Copy of Article Publication Available : www.ijmer.in
https://doi.org/ijmer.in/14.08(1)/2025.33

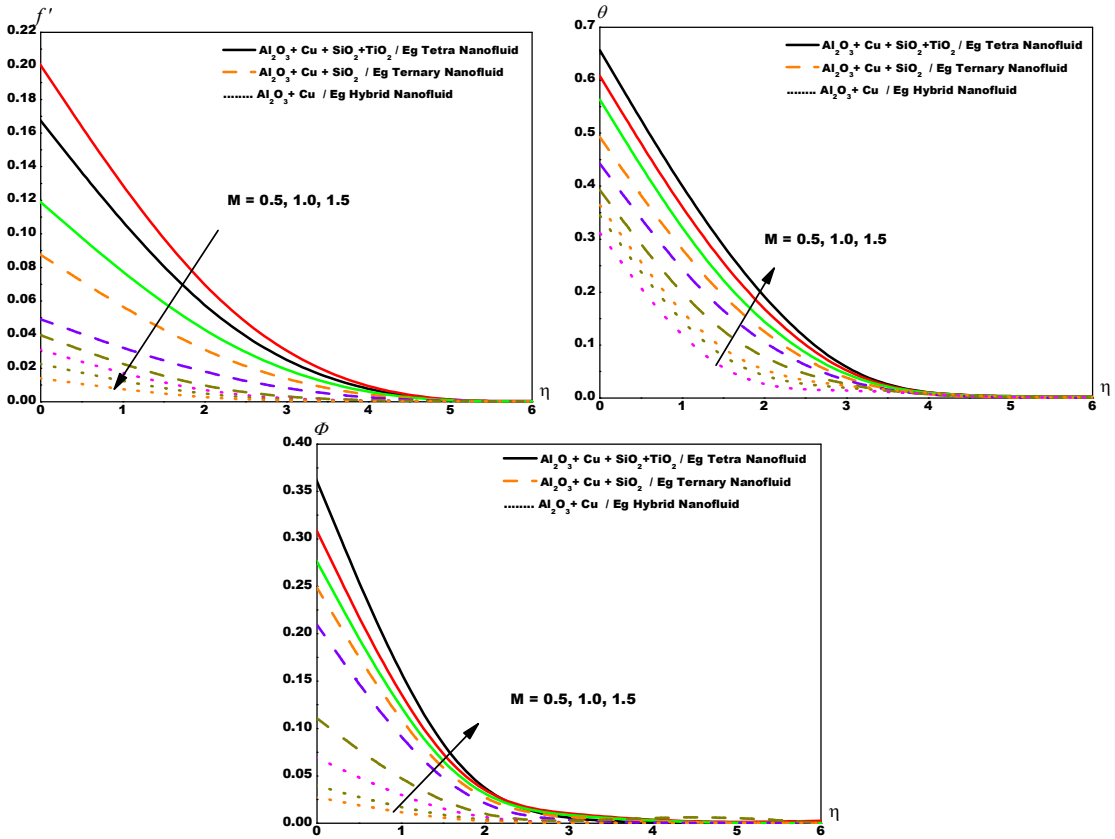


Fig.4 : Impact on Magnetic parameter (M) of [a] f', [b] θ, [c] Φ

Cover Page

INTERNATIONAL JOURNAL OF MULTIDISCIPLINARY EDUCATIONAL RESEARCH
ISSN:2277-7881(Print); IMPACT FACTOR :9.014(2025); IC VALUE:5.16; ISI VALUE:2.286
PEER REVIEWED AND REFEREED INTERNATIONAL JOURNAL
(Fulfilled Suggests Parameters of UGC by IJMER)
Volume:14, Issue:8(1), August, 2025
Scopus Review ID: A2B96D3ACF3FEA2A
Article Received: Reviewed : Accepted
Publisher: Sucharitha Publication, India
Online Copy of Article Publication Available : www.ijmer.in
https://doi.org/ijmer.in/14.08(1)/2025.33

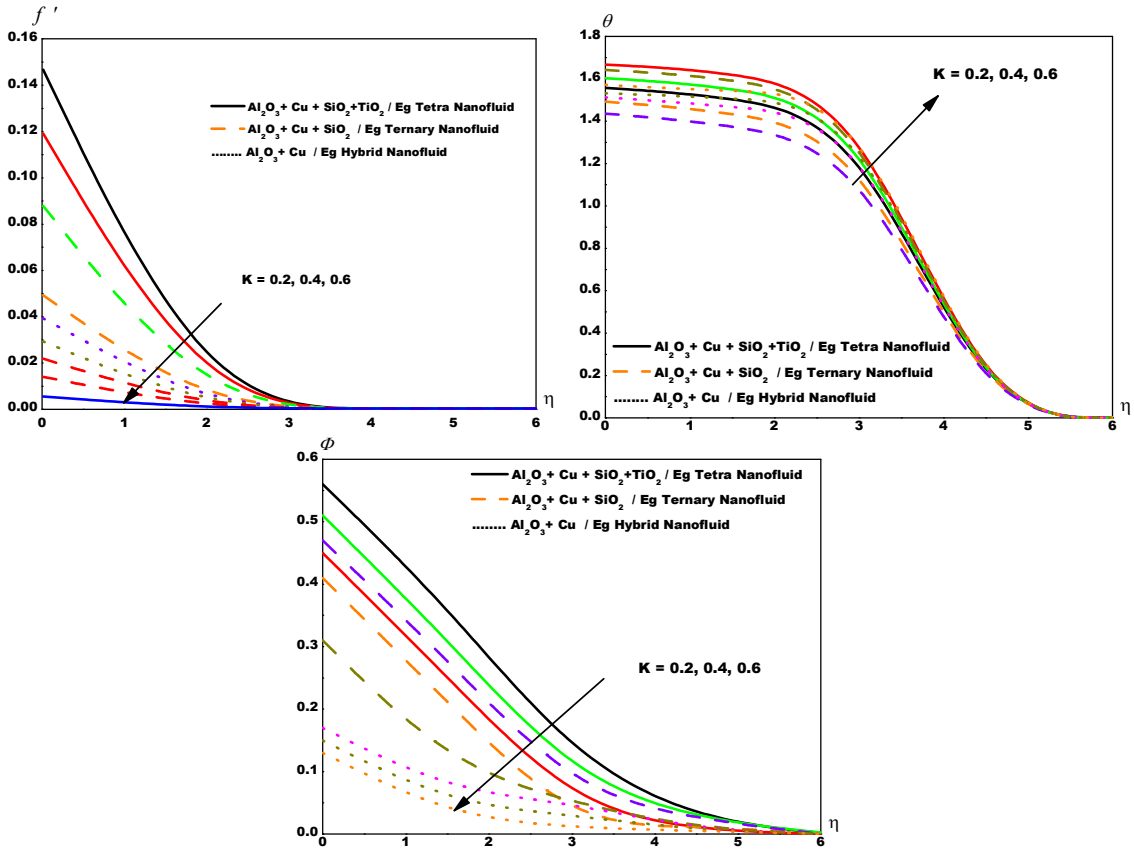


Fig.5 : Impact on Inverse Darcy parameter(K) of [a] f', [b] θ, [c] Φ

Cover Page

INTERNATIONAL JOURNAL OF MULTIDISCIPLINARY EDUCATIONAL RESEARCH
ISSN:2277-7881(Print); IMPACT FACTOR :9.014(2025); IC VALUE:5.16; ISI VALUE:2.286
PEER REVIEWED AND REFEREED INTERNATIONAL JOURNAL
(Fulfilled Suggests Parameters of UGC by IJMER)
Volume:14, Issue:8(1), August, 2025
Scopus Review ID: A2B96D3ACF3FEA2A
Article Received: Reviewed : Accepted
Publisher: Sucharitha Publication, India
Online Copy of Article Publication Available : www.ijmer.in
https://doi.org/ijmer.in/14.08(1)/2025.33

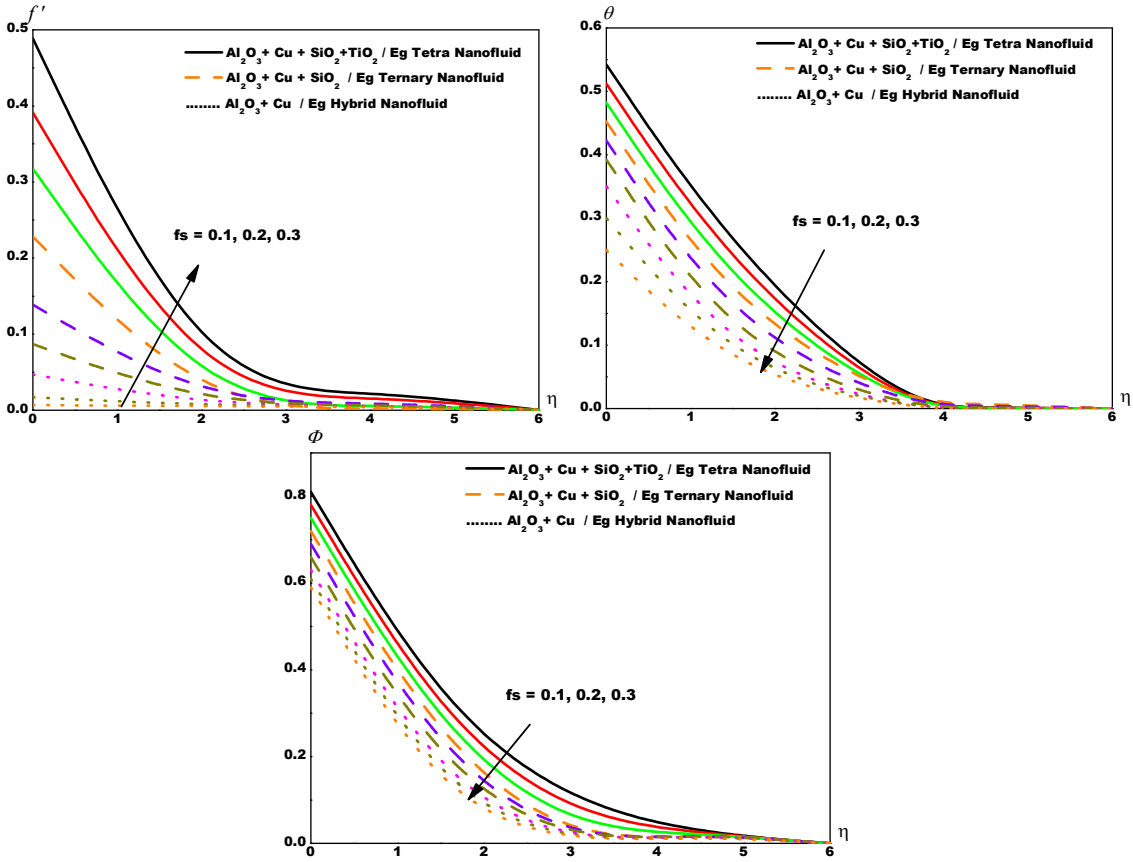


Fig.6 : Impact on Forchheimer parameter(fs) of [a] f', [b] θ, [c] Φ

Cover Page

INTERNATIONAL JOURNAL OF MULTIDISCIPLINARY EDUCATIONAL RESEARCH
ISSN:2277-7881(Print); IMPACT FACTOR :9.014(2025); IC VALUE:5.16; ISI VALUE:2.286
PEER REVIEWED AND REFEREED INTERNATIONAL JOURNAL
(Fulfilled Suggests Parameters of UGC by IJMER)
Volume:14, Issue:8(1), August, 2025
Scopus Review ID: A2B96D3ACF3FEA2A
Article Received: Reviewed : Accepted
Publisher: Sucharitha Publication, India
Online Copy of Article Publication Available : www.ijmer.in
https://doi.org/ijmer.in/14.08(1)/2025.33

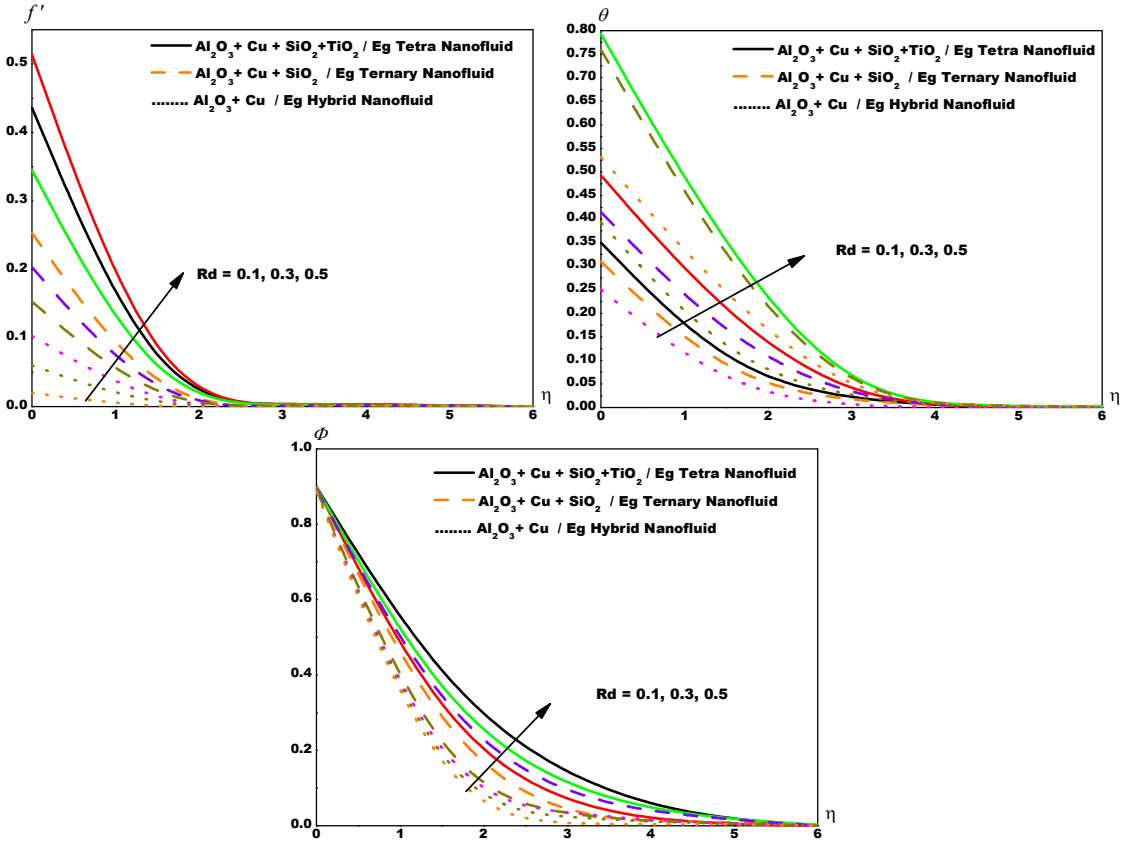


Fig.7 : Impact on Radiation parameter(Rd) of [a] f', [b] θ, [c] Φ

Cover Page

INTERNATIONAL JOURNAL OF MULTIDISCIPLINARY EDUCATIONAL RESEARCH
ISSN:2277-7881(Print); IMPACT FACTOR :9.014(2025); IC VALUE:5.16; ISI VALUE:2.286
PEER REVIEWED AND REFEREED INTERNATIONAL JOURNAL
(Fulfilled Suggests Parameters of UGC by IJMER)
Volume:14, Issue:8(1), August, 2025
Scopus Review ID: A2B96D3ACF3FEA2A
Article Received: Reviewed : Accepted
Publisher: Sucharitha Publication, India
Online Copy of Article Publication Available : www.ijmer.in
https://doi.org/ijmer.in/14.08(1)/2025.33

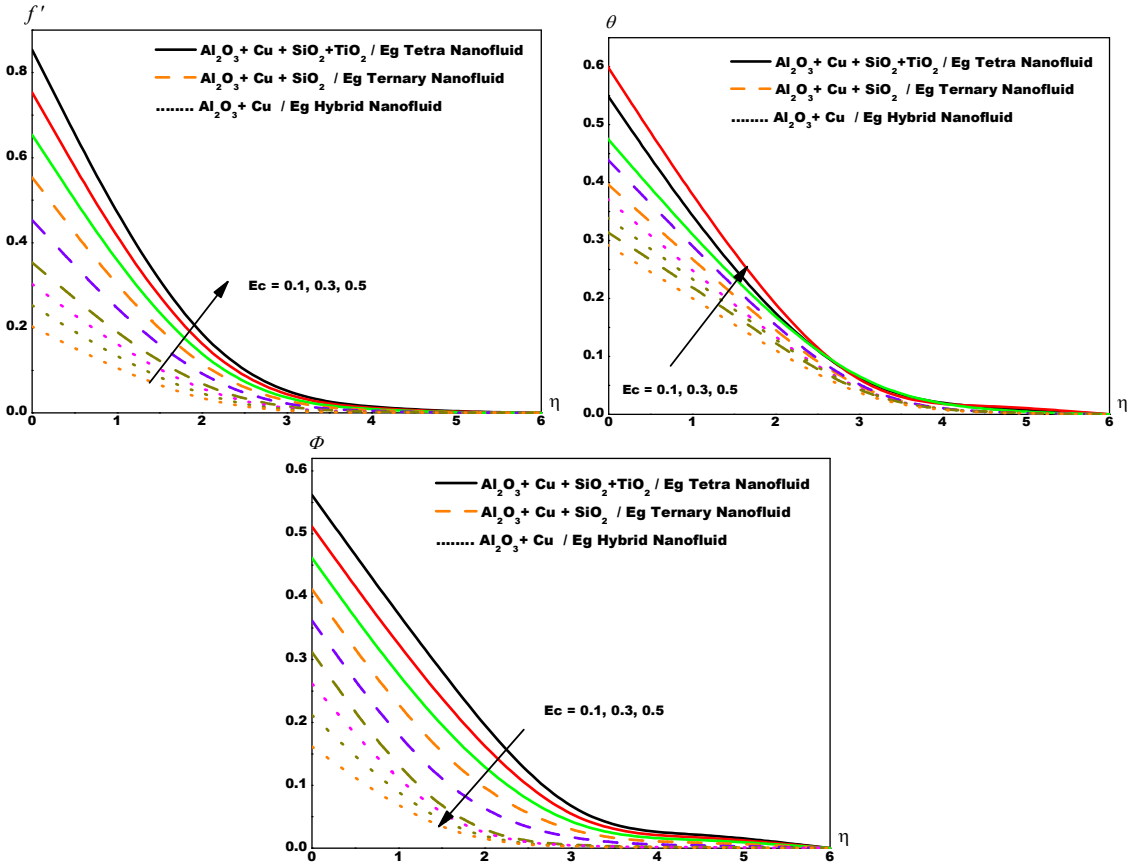


Fig.8 : Impact on Eckert number(Ec) of [a] f', [b] θ, [c] Φ

Cover Page

INTERNATIONAL JOURNAL OF MULTIDISCIPLINARY EDUCATIONAL RESEARCH
ISSN:2277-7881(Print); IMPACT FACTOR :9.014(2025); IC VALUE:5.16; ISI VALUE:2.286
PEER REVIEWED AND REFEREED INTERNATIONAL JOURNAL
(Fulfilled Suggests Parameters of UGC by IJMER)
Volume:14, Issue:8(1), August, 2025
Scopus Review ID: A2B96D3ACF3FEA2A
Article Received: Reviewed : Accepted
Publisher: Sucharitha Publication, India
Online Copy of Article Publication Available : www.ijmer.in
https://doi.org/ijmer.in/14.08(1)/2025.33

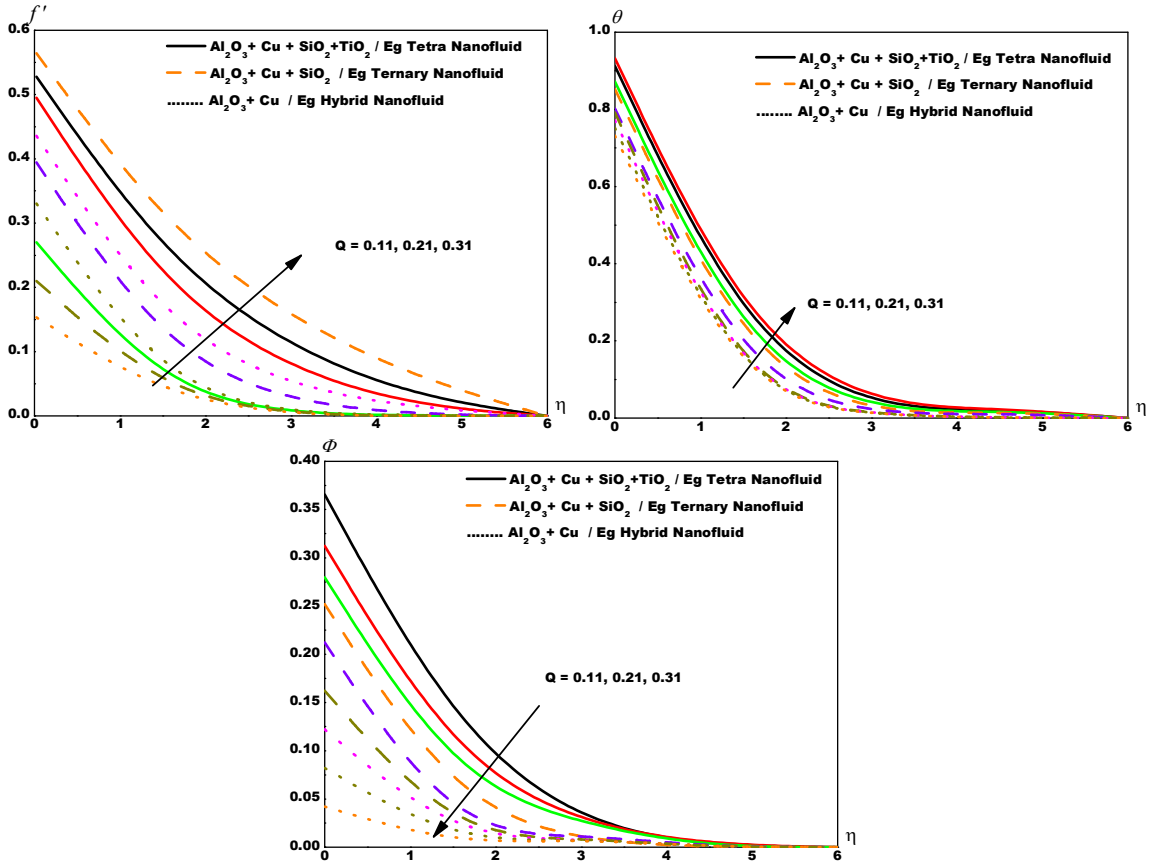


Fig.9 : Impact on Heat Source Parameter(Q) of [a] f', [b] θ, [c] Φ

Cover Page

INTERNATIONAL JOURNAL OF MULTIDISCIPLINARY EDUCATIONAL RESEARCH
ISSN:2277-7881(Print); IMPACT FACTOR :9.014(2025); IC VALUE:5.16; ISI VALUE:2.286
PEER REVIEWED AND REFEREED INTERNATIONAL JOURNAL
(Fulfilled Suggests Parameters of UGC by IJMER)
Volume:14, Issue:8(1), August, 2025
Scopus Review ID: A2B96D3ACF3FEA2A
Article Received: Reviewed : Accepted
Publisher: Sucharitha Publication, India
Online Copy of Article Publication Available : www.ijmer.in
https://doi.org/ijmer.in/14.08(1)/2025.33

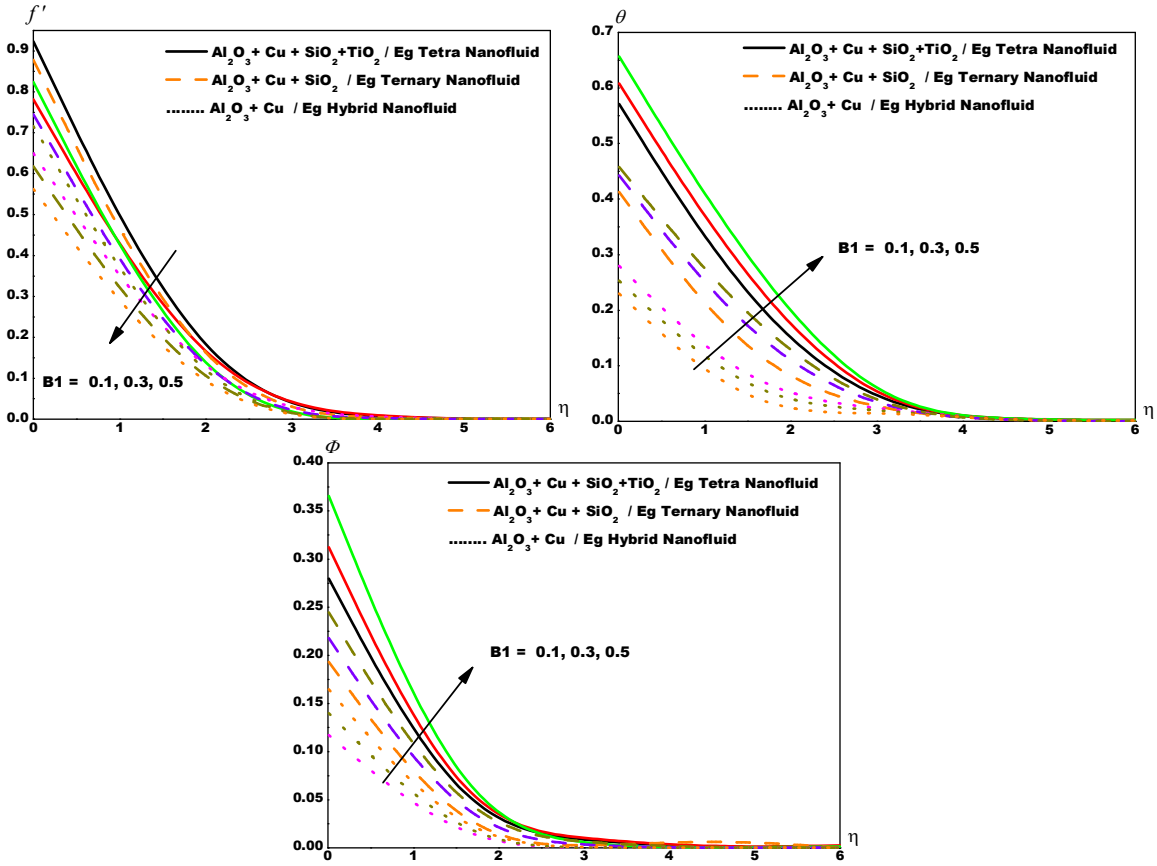


Fig.10 : Impact on Velocity Slip(B1) of [a] f', [b] θ, [c] Φ

Cover Page

INTERNATIONAL JOURNAL OF MULTIDISCIPLINARY EDUCATIONAL RESEARCH
ISSN:2277-7881(Print); IMPACT FACTOR :9.014(2025); IC VALUE:5.16; ISI VALUE:2.286
PEER REVIEWED AND REFEREED INTERNATIONAL JOURNAL
(Fulfilled Suggests Parameters of UGC by IJMER)
Volume:14, Issue:8(1), August, 2025
Scopus Review ID: A2B96D3ACF3FEA2A
Article Received: Reviewed : Accepted
Publisher: Sucharitha Publication, India
Online Copy of Article Publication Available : www.ijmer.in
https://doi.org/ijmer.in/14.08(1)/2025.33

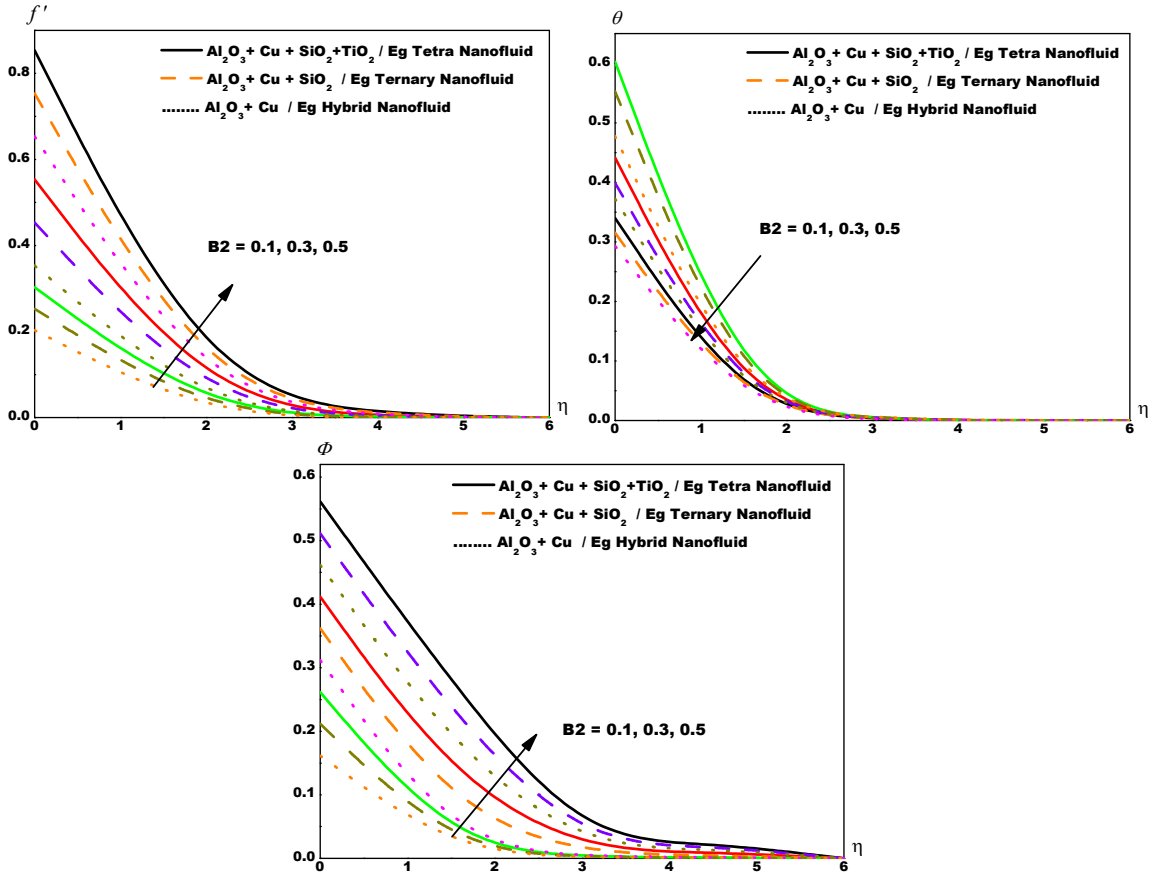


Fig.11 : Impact on Thermal slip(B2) of [a] f', [b] θ, [c] Φ

Cover Page

INTERNATIONAL JOURNAL OF MULTIDISCIPLINARY EDUCATIONAL RESEARCH
ISSN:2277-7881(Print); IMPACT FACTOR :9.014(2025); IC VALUE:5.16; ISI VALUE:2.286
PEER REVIEWED AND REFEREED INTERNATIONAL JOURNAL
(Fulfilled Suggests Parameters of UGC by IJMER)
Volume:14, Issue:8(1), August, 2025
Scopus Review ID: A2B96D3ACF3FEA2A
Article Received: Reviewed : Accepted
Publisher: Sucharitha Publication, India
Online Copy of Article Publication Available : www.ijmer.in
https://doi.org/ijmer.in/14.08(1)/2025.33

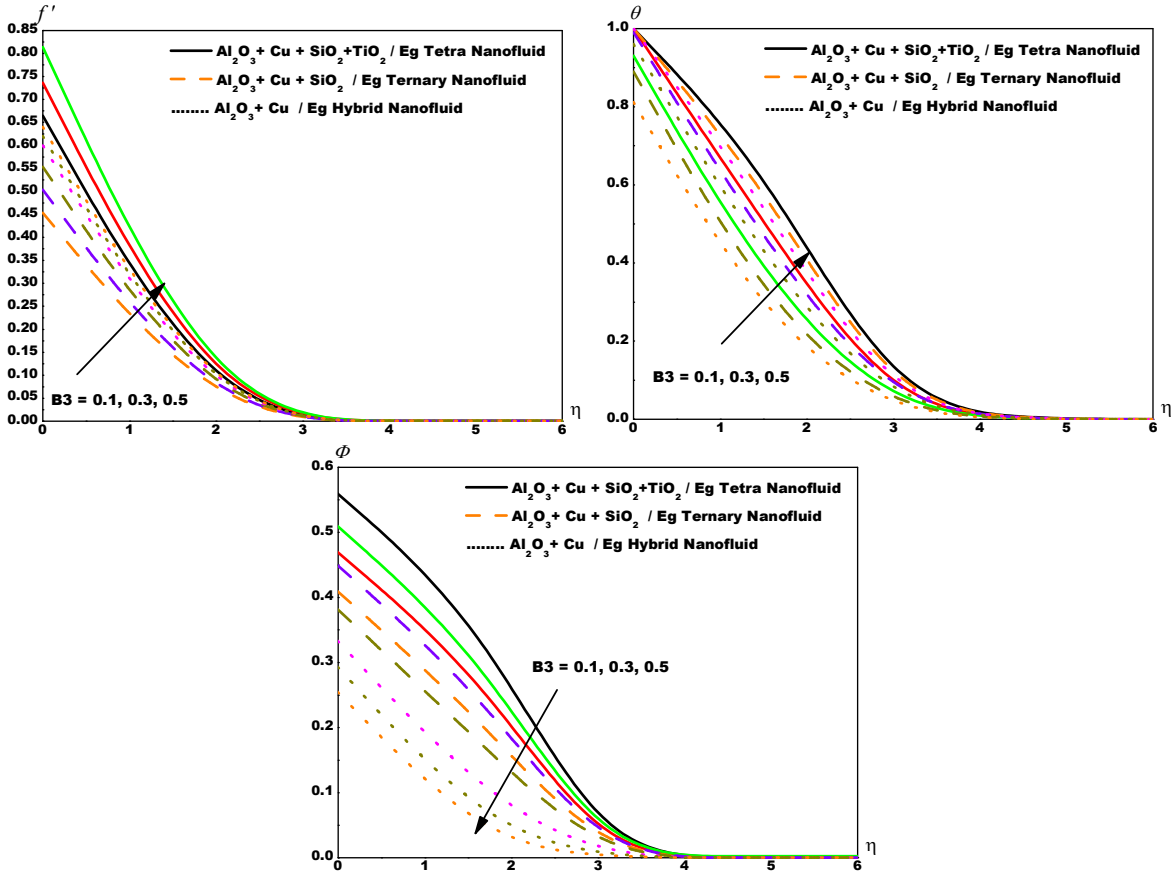


Fig.12 : Impact on Solutal slip(B3) of [a] f', [b] θ, [c] Φ

Cover Page

INTERNATIONAL JOURNAL OF MULTIDISCIPLINARY EDUCATIONAL RESEARCH
ISSN:2277-7881(Print); IMPACT FACTOR :9.014(2025); IC VALUE:5.16; ISI VALUE:2.286
PEER REVIEWED AND REFEREED INTERNATIONAL JOURNAL
(Fulfilled Suggests Parameters of UGC by IJMER)
Volume:14, Issue:8(1), August, 2025
Scopus Review ID: A2B96D3ACF3FEA2A
Article Received: Reviewed : Accepted
Publisher: Sucharitha Publication, India
Online Copy of Article Publication Available : www.ijmer.in
https://doi.org/ijmer.in/14.08(1)/2025.33

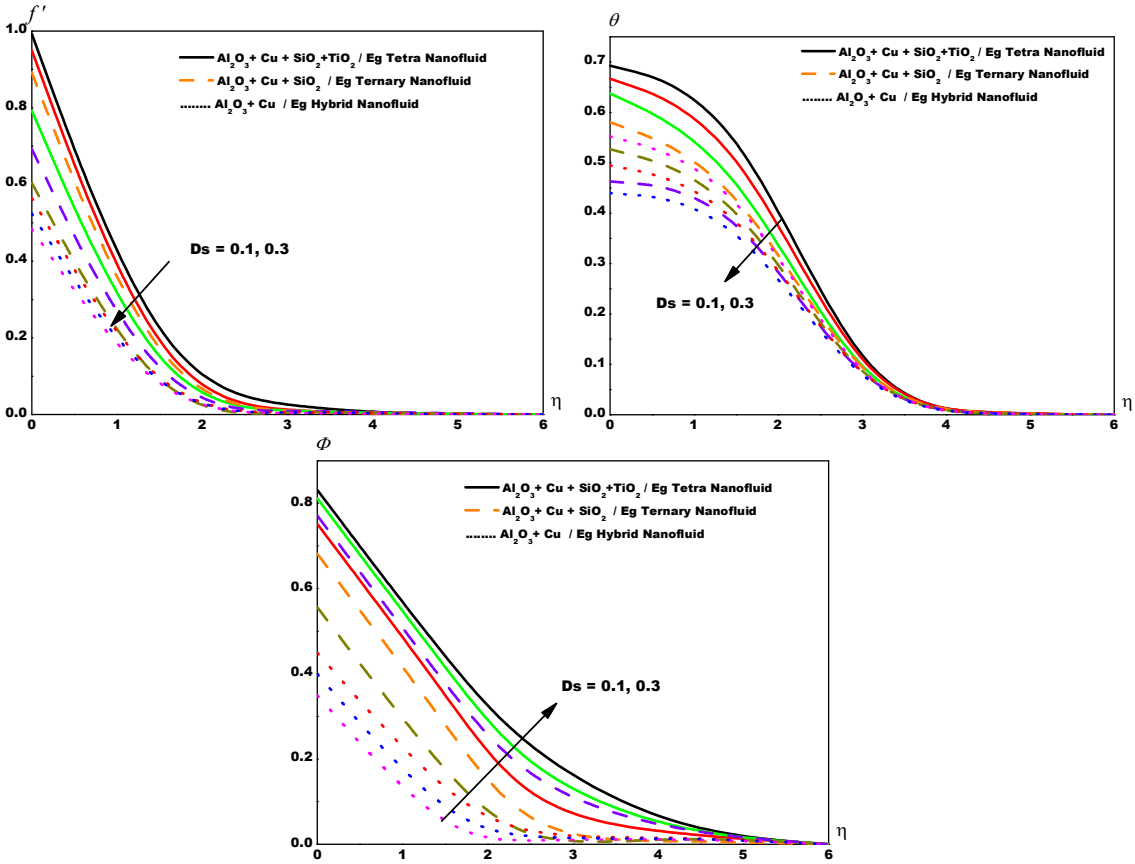


Fig.13 : Impact on Thermal dispersion(Ds) parameter of [a] f', [b] θ, [c] Φ

Cover Page

INTERNATIONAL JOURNAL OF MULTIDISCIPLINARY EDUCATIONAL RESEARCH
ISSN:2277-7881(Print); IMPACT FACTOR :9.014(2025); IC VALUE:5.16; ISI VALUE:2.286
PEER REVIEWED AND REFEREED INTERNATIONAL JOURNAL
(Fulfilled Suggests Parameters of UGC by IJMER)
Volume:14, Issue:8(1), August, 2025
Scopus Review ID: A2B96D3ACF3FEA2A
Article Received: Reviewed : Accepted
Publisher: Sucharitha Publication, India
Online Copy of Article Publication Available : www.ijmer.in
https://doi.org/ijmer.in/14.08(1)/2025.33

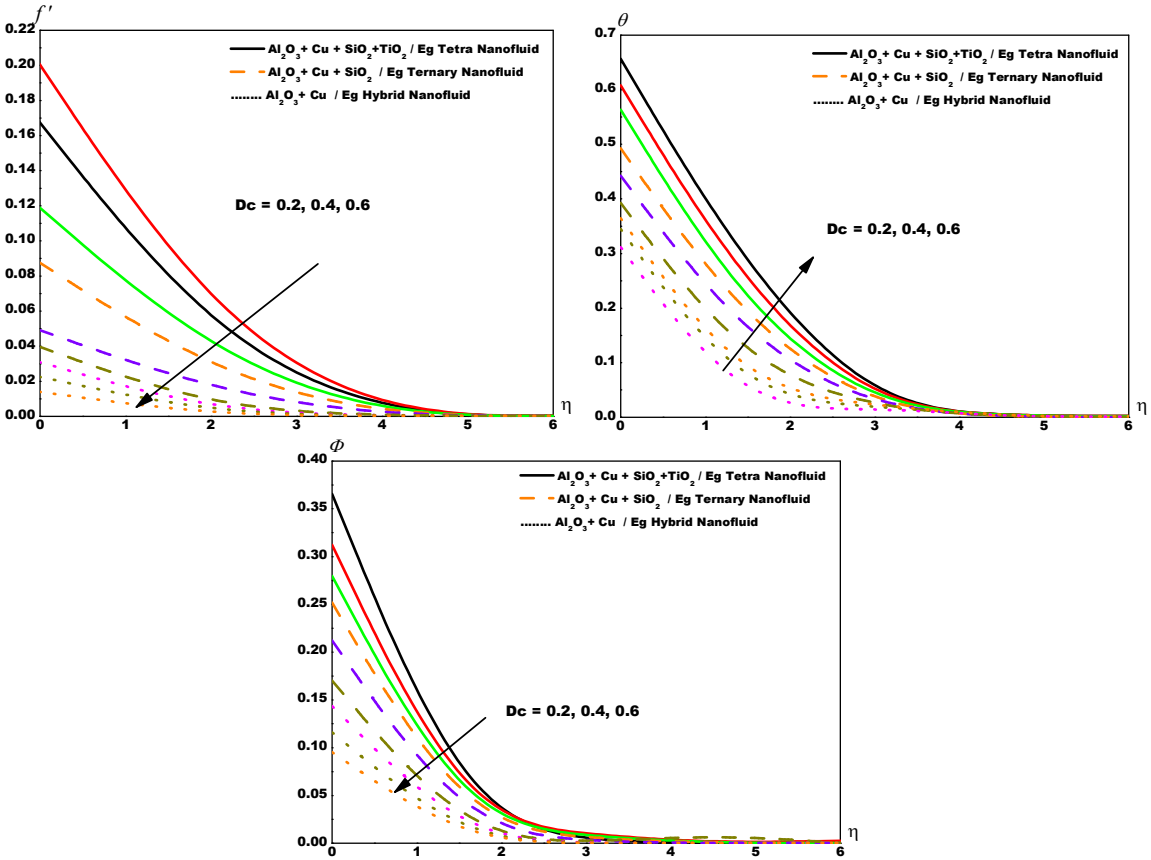


Fig.14 : Impact on solutal dispersion (Dc) parameter of [a] f', [b] θ, [c] Φ

Cover Page

INTERNATIONAL JOURNAL OF MULTIDISCIPLINARY EDUCATIONAL RESEARCH
ISSN:2277-7881(Print); IMPACT FACTOR :9.014(2025); IC VALUE:5.16; ISI VALUE:2.286
PEER REVIEWED AND REFEREED INTERNATIONAL JOURNAL
(Fulfilled Suggests Parameters of UGC by IJMER)
Volume:14, Issue:8(1), August, 2025
Scopus Review ID: A2B96D3ACF3FEA2A
Article Received: Reviewed : Accepted
Publisher: Sucharitha Publication, India
Online Copy of Article Publication Available : www.ijmer.in
https://doi.org/ijmer.in/14.08(1)/2025.33

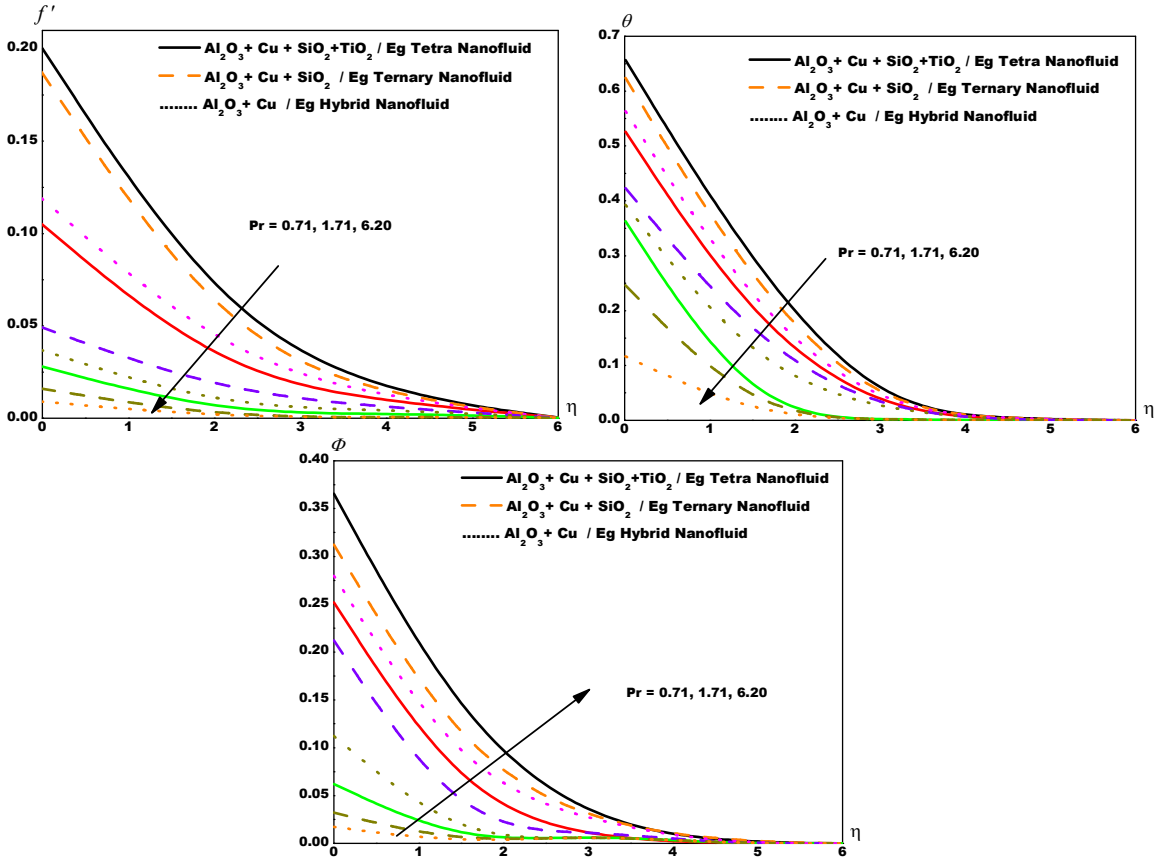


Fig.15 : Impact on Prandtl number(Pr) of [a] f', [b] θ, [c] Φ

Cover Page

INTERNATIONAL JOURNAL OF MULTIDISCIPLINARY EDUCATIONAL RESEARCH
ISSN:2277-7881(Print); IMPACT FACTOR :9.014(2025); IC VALUE:5.16; ISI VALUE:2.286
PEER REVIEWED AND REFEREED INTERNATIONAL JOURNAL
(Fulfilled Suggests Parameters of UGC by IJMER)
Volume:14, Issue:8(1), August, 2025
Scopus Review ID: A2B96D3ACF3FEA2A
Article Received: Reviewed : Accepted
Publisher: Sucharitha Publication, India
Online Copy of Article Publication Available : www.ijmer.in
https://doi.org/ijmer.in/14.08(1)/2025.33

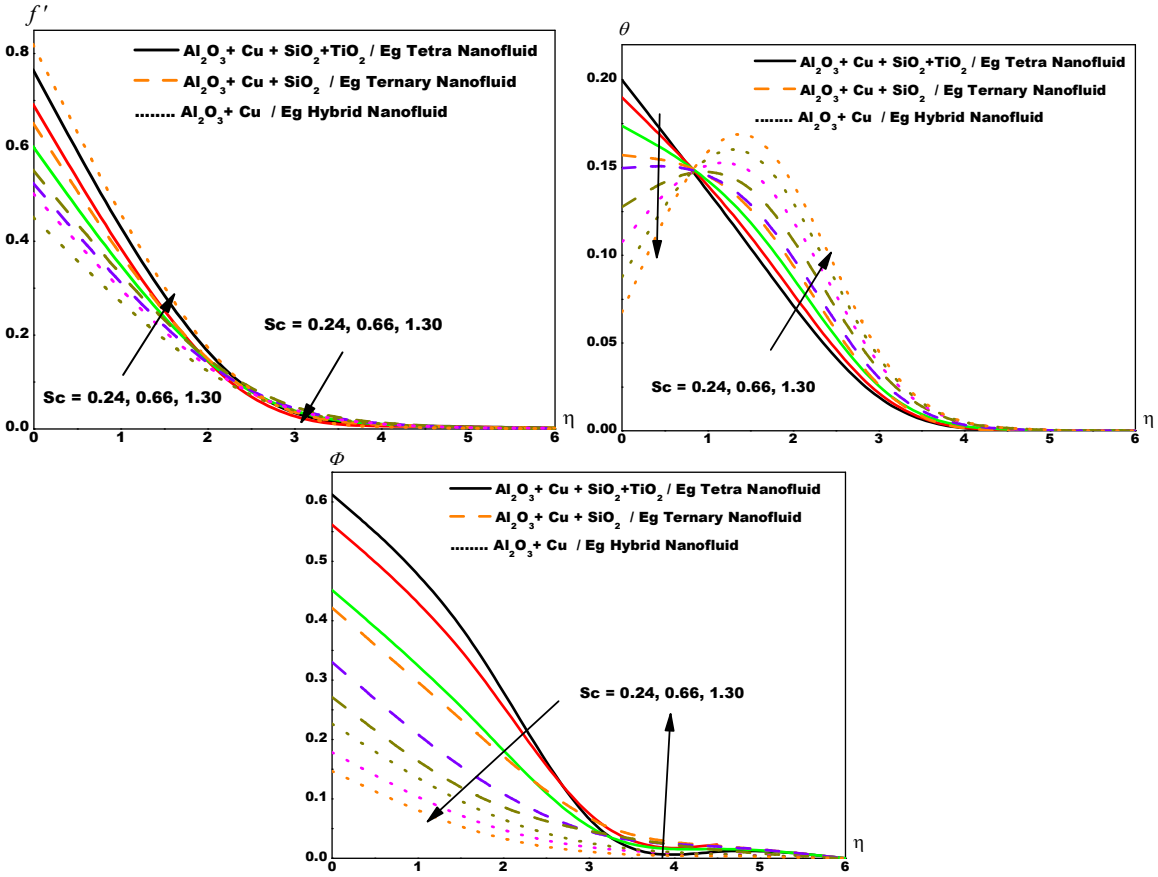


Fig.16 : Impact on Schmidt number(Sc) of [a] f', [b] θ, [c] Φ

Cover Page

INTERNATIONAL JOURNAL OF MULTIDISCIPLINARY EDUCATIONAL RESEARCH
ISSN:2277-7881(Print); IMPACT FACTOR :9.014(2025); IC VALUE:5.16; ISI VALUE:2.286
PEER REVIEWED AND REFEREED INTERNATIONAL JOURNAL
(Fulfilled Suggests Parameters of UGC by IJMER)
Volume:14, Issue:8(1), August, 2025
Scopus Review ID: A2B96D3ACF3FEA2A
Article Received: Reviewed : Accepted
Publisher: Sucharitha Publication, India
Online Copy of Article Publication Available : www.ijmer.in
https://doi.org/ijmer.in/14.08(1)/2025.33

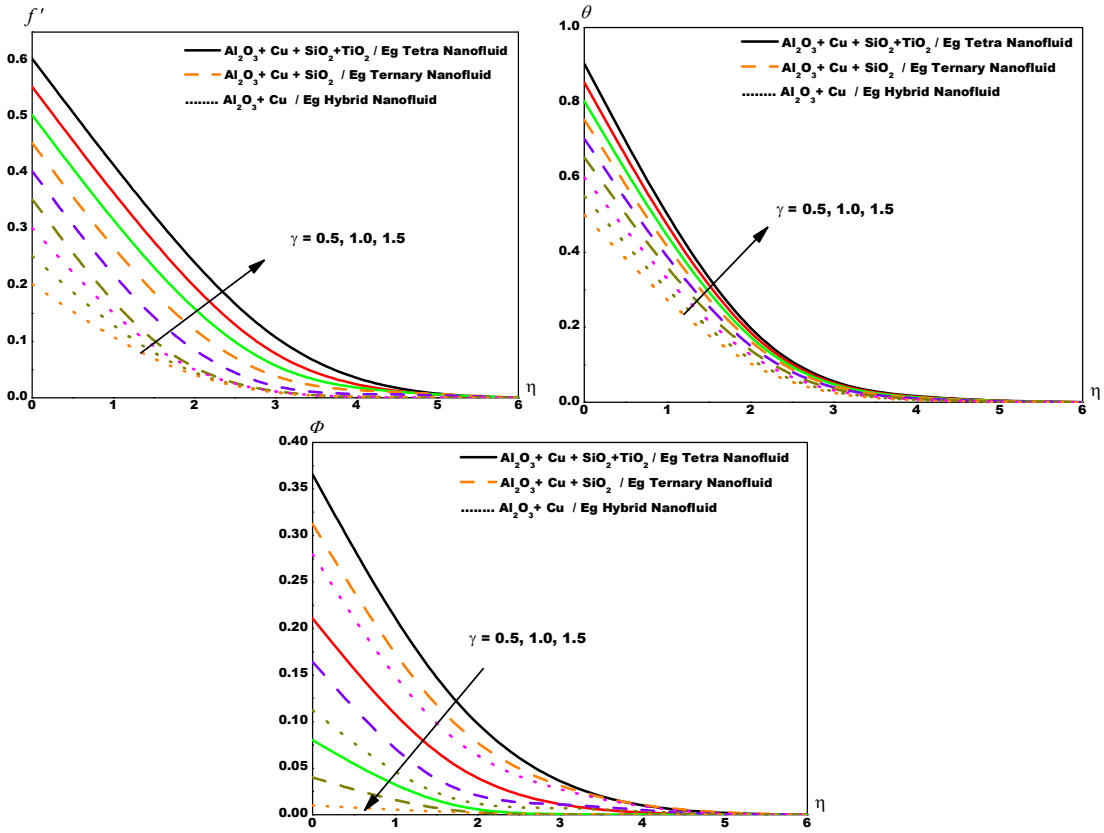


Fig.17 : Impact on Chemical Reaction(γ) of [a] f', [b] θ, [c] Φ

Cover Page

INTERNATIONAL JOURNAL OF MULTIDISCIPLINARY EDUCATIONAL RESEARCH
ISSN:2277-7881(Print); IMPACT FACTOR :9.014(2025); IC VALUE:5.16; ISI VALUE:2.286
PEER REVIEWED AND REFEREED INTERNATIONAL JOURNAL
(Fulfilled Suggests Parameters of UGC by IJMER)
Volume:14, Issue:8(1), August, 2025
Scopus Review ID: A2B96D3ACF3FEA2A
Article Received: Reviewed : Accepted
Publisher: Sucharitha Publication, India
Online Copy of Article Publication Available : www.ijmer.in
https://doi.org/ijmer.in/14.08(1)/2025.33

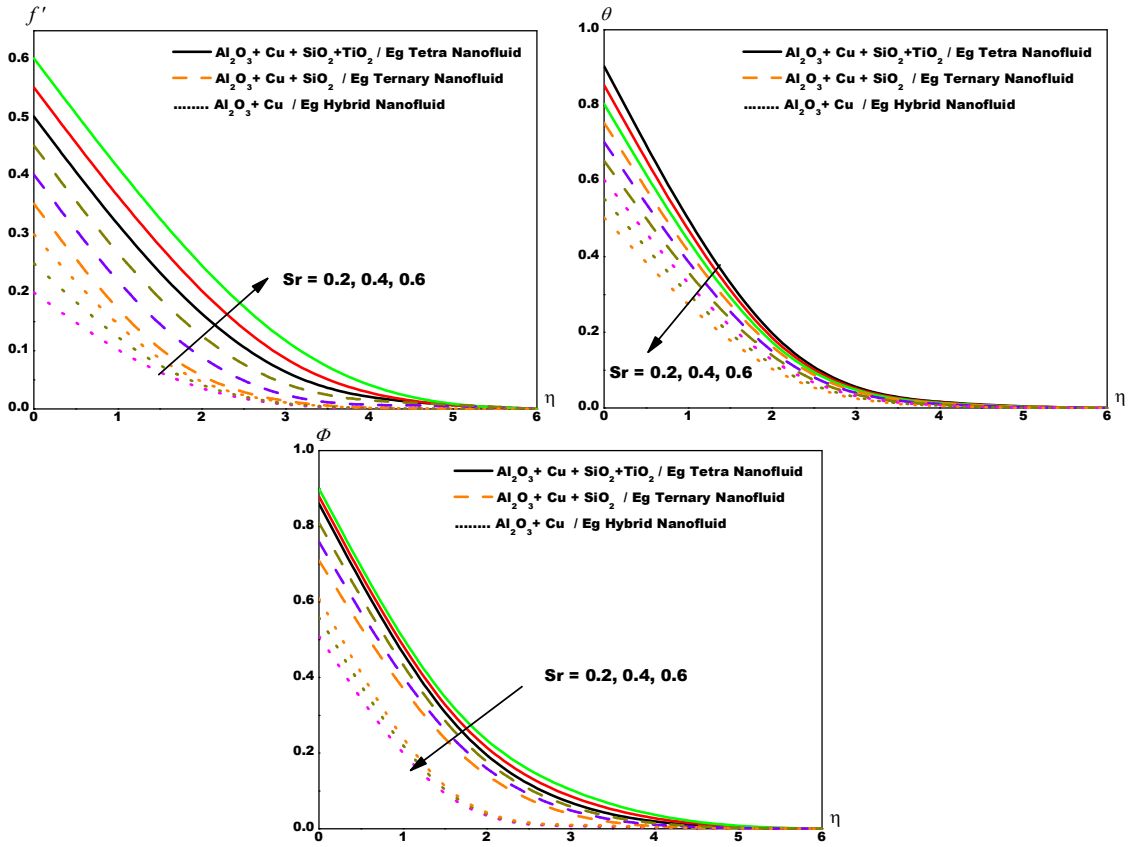


Fig.18 : Impact on Soret(Sr) parameter of [a] f', [b] θ, [c] Φ

Cover Page

INTERNATIONAL JOURNAL OF MULTIDISCIPLINARY EDUCATIONAL RESEARCH
ISSN:2277-7881(Print); IMPACT FACTOR :9.014(2025); IC VALUE:5.16; ISI VALUE:2.286
PEER REVIEWED AND REFEREED INTERNATIONAL JOURNAL
(Fulfilled Suggests Parameters of UGC by IJMER)
Volume:14, Issue:8(1), August, 2025
Scopus Review ID: A2B96D3ACF3FEA2A
Article Received: Reviewed : Accepted
Publisher: Sucharitha Publication, India
Online Copy of Article Publication Available : www.ijmer.in
https://doi.org/ijmer.in/14.08(1)/2025.33

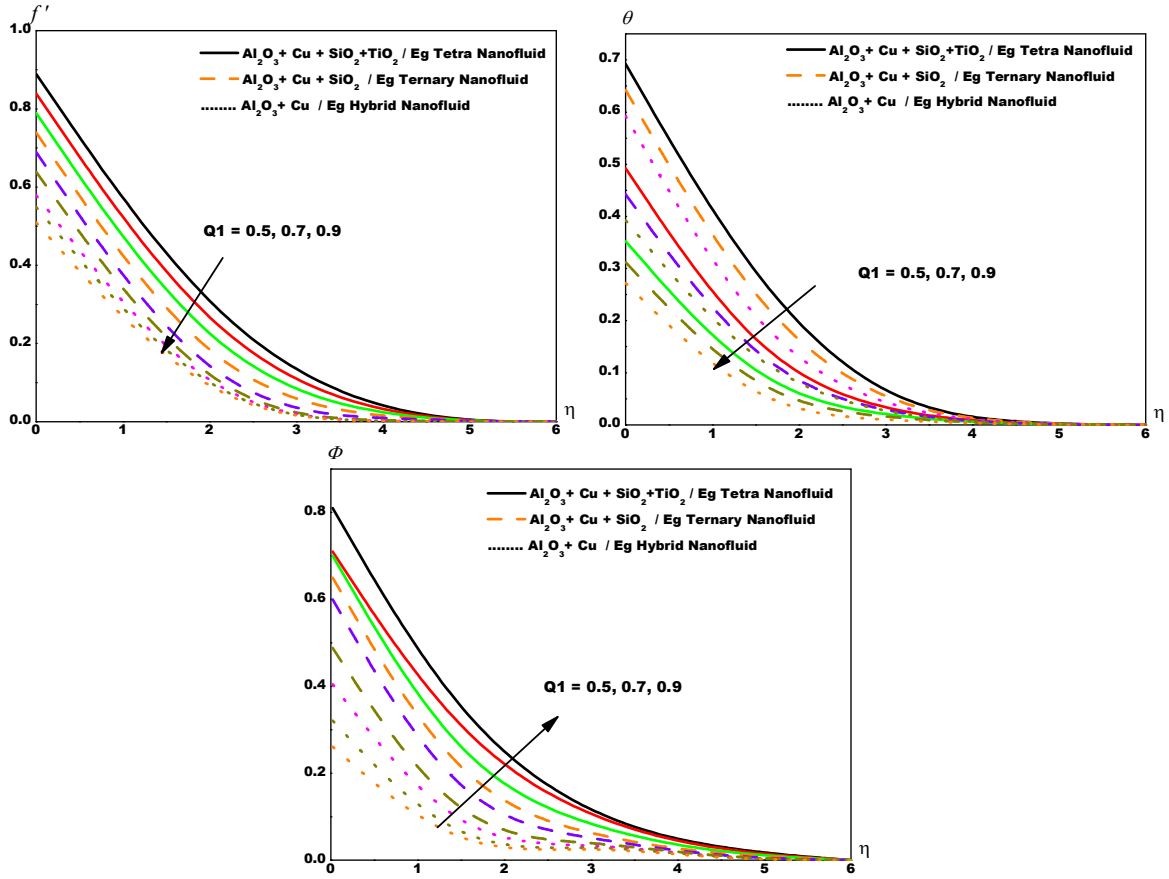


Fig.19 : Impact on Reaction rate (Exothermic chemical reaction) (Q1) of [a] f', [b] θ, [c] Φ

Cover Page

INTERNATIONAL JOURNAL OF MULTIDISCIPLINARY EDUCATIONAL RESEARCH
ISSN:2277-7881(Print); IMPACT FACTOR :9.014(2025); IC VALUE:5.16; ISI VALUE:2.286
PEER REVIEWED AND REFEREED INTERNATIONAL JOURNAL
(Fulfilled Suggests Parameters of UGC by IJMER)
Volume:14, Issue:8(1), August, 2025
Scopus Review ID: A2B96D3ACF3FEA2A
Article Received: Reviewed : Accepted
Publisher: Sucharitha Publication, India
Online Copy of Article Publication Available : www.ijmer.in
https://doi.org/ijmer.in/14.08(1)/2025.33

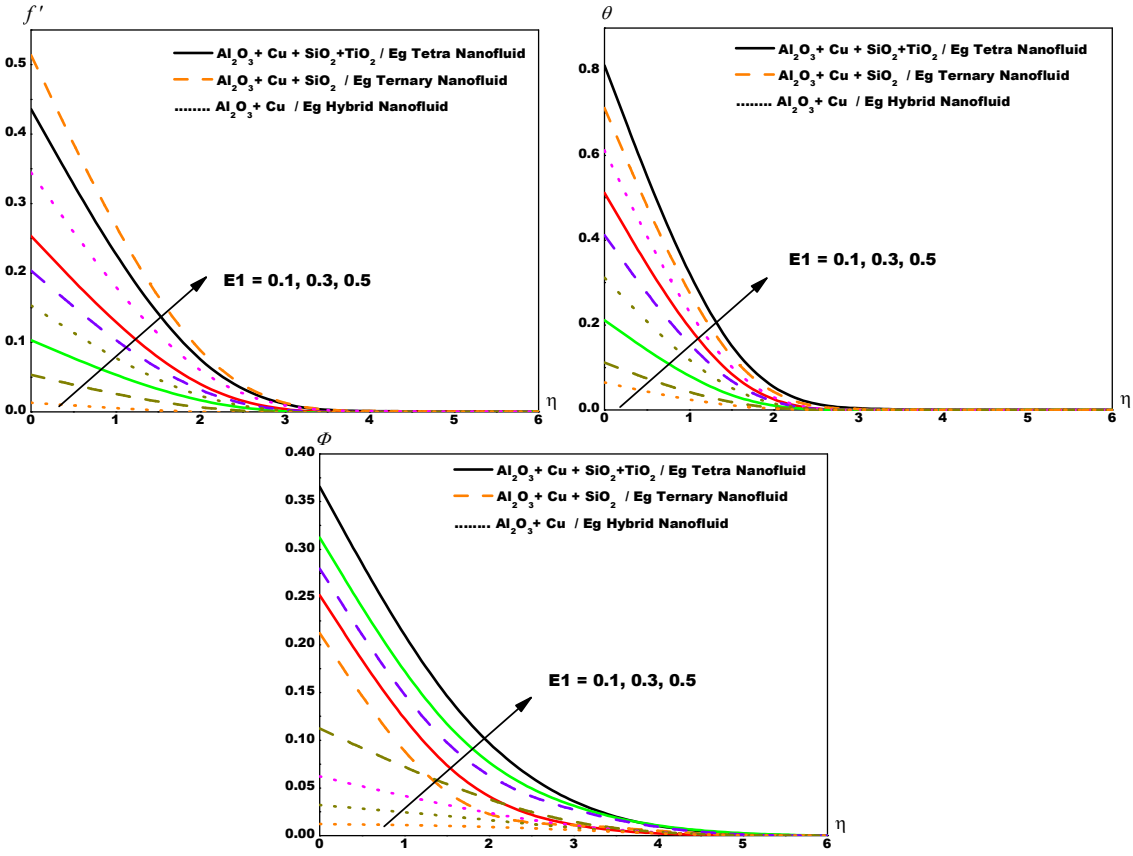


Fig.20 : Impact on Activation Energy(E1) of [a] f', [b] θ, [c] Φ

Cover Page

INTERNATIONAL JOURNAL OF MULTIDISCIPLINARY EDUCATIONAL RESEARCH
ISSN:2277-7881(Print); IMPACT FACTOR :9.014(2025); IC VALUE:5.16; ISI VALUE:2.286
PEER REVIEWED AND REFEREED INTERNATIONAL JOURNAL
(Fulfilled Suggests Parameters of UGC by IJMER)
Volume:14, Issue:8(1), August, 2025
Scopus Review ID: A2B96D3ACF3FEA2A
Article Received: Reviewed : Accepted
Publisher: Sucharitha Publication, India
Online Copy of Article Publication Available : www.ijmer.in
https://doi.org/ijmer.in/14.08(1)/2025.33

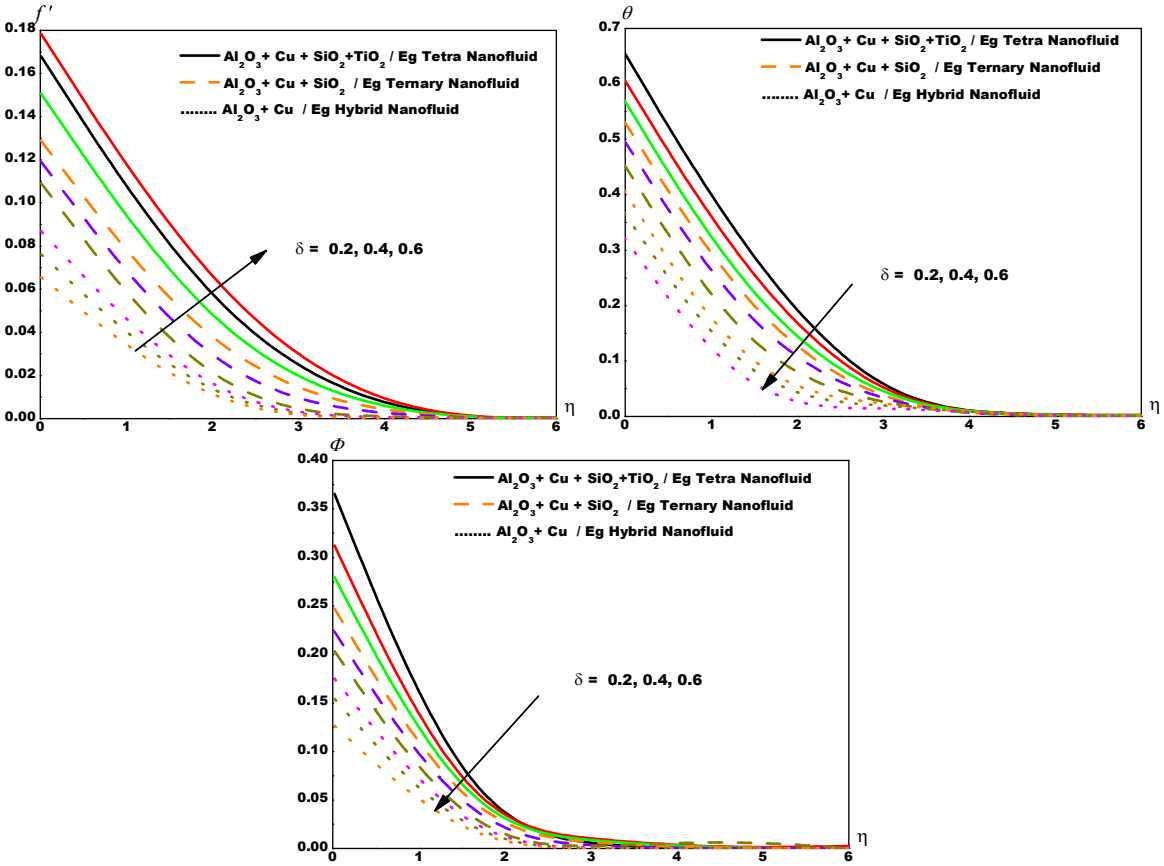


Fig.21 : Impact on Temperature difference ratio(δ) of [a] f', [b] θ, [c] Φ

Cover Page

INTERNATIONAL JOURNAL OF MULTIDISCIPLINARY EDUCATIONAL RESEARCH
ISSN:2277-7881(Print); IMPACT FACTOR :9.014(2025); IC VALUE:5.16; ISI VALUE:2.286
PEER REVIEWED AND REFEREED INTERNATIONAL JOURNAL
(Fulfilled Suggests Parameters of UGC by IJMER)
Volume:14, Issue:8(1), August, 2025
Scopus Review ID: A2B96D3ACF3FEA2A
Article Received: Reviewed : Accepted
Publisher: Sucharitha Publication, India
Online Copy of Article Publication Available : www.ijmer.in
https://doi.org/ijmer.in/14.08(1)/2025.33

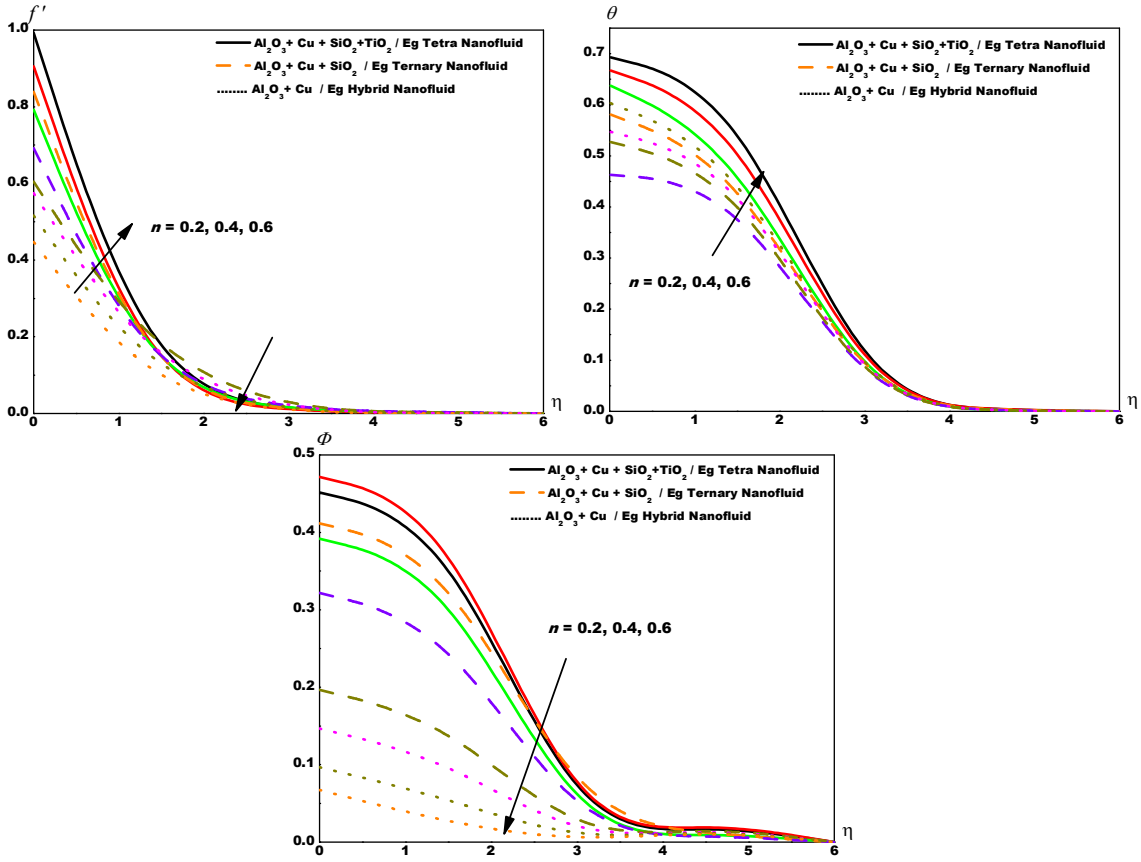


Fig.22 : Impact on Index(n) parameter of [a] f', [b] θ, [c] Φ

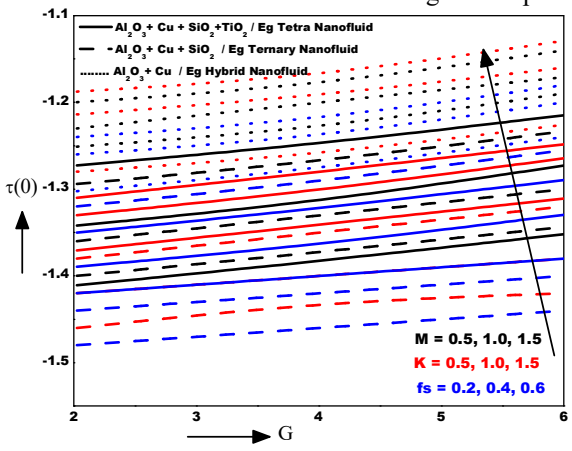


Fig.23 : Impression of G,M, K, fs on τ

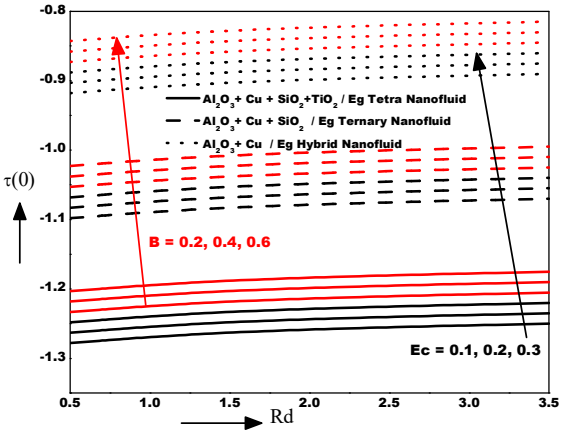


Fig.24 : Impact of Rd, Ec, B on τ

Cover Page

INTERNATIONAL JOURNAL OF MULTIDISCIPLINARY EDUCATIONAL RESEARCH
ISSN:2277-7881(Print); IMPACT FACTOR :9.014(2025); IC VALUE:5.16; ISI VALUE:2.286
PEER REVIEWED AND REFEREED INTERNATIONAL JOURNAL
(Fulfilled Suggests Parameters of UGC by IJMER)
Volume:14, Issue:8(1), August, 2025
Scopus Review ID: A2B96D3ACF3FEA2A
Article Received: Reviewed : Accepted
Publisher: Sucharitha Publication, India
Online Copy of Article Publication Available : www.ijmer.in
https://doi.org/ijmer.in/14.08(1)/2025.33

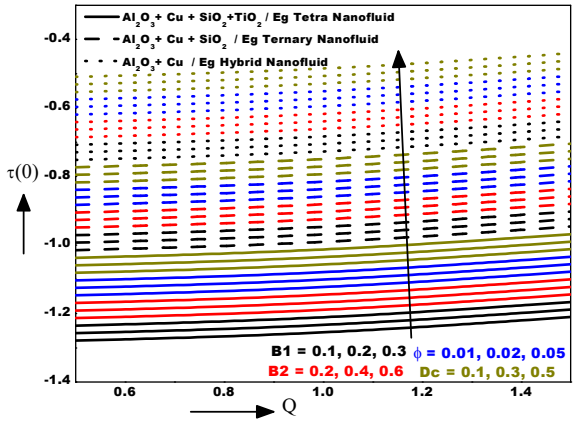


Fig.25: Control of Q, B1, B2, ϕ, Dc on τ

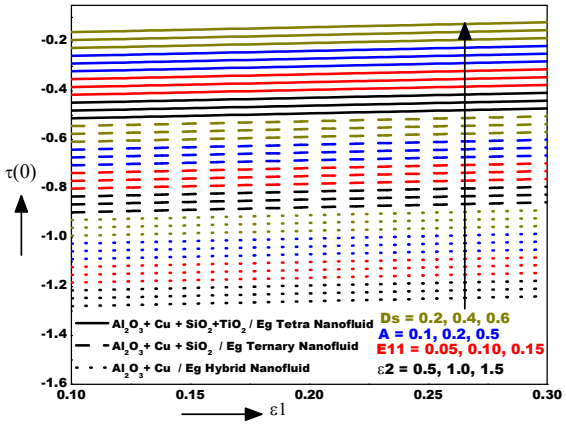


Fig.26 : Impact on ε1, ε2, E11, A, Ds of τ = 0

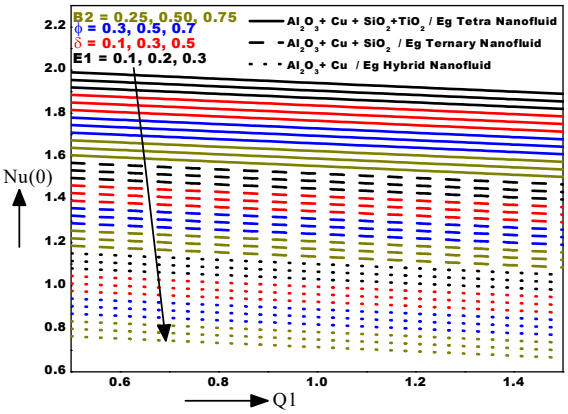


Fig.26: Variation on Q1, E1, δ, ϕ, B2 on Nu

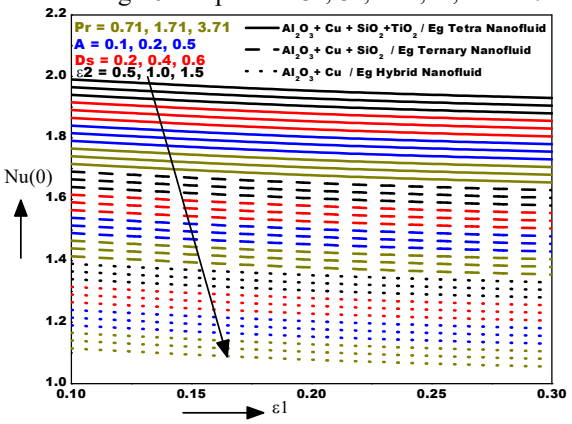


Fig.29 : Impression on ε1, ε2, Ds, A, Pr of Nu = 0

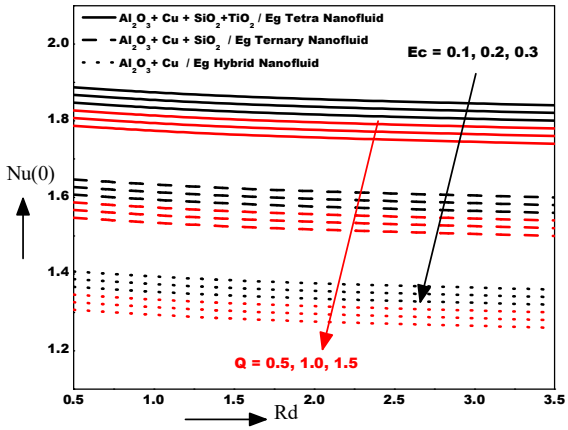


Fig.27 :Control on Rd, Ec, Q on Nu

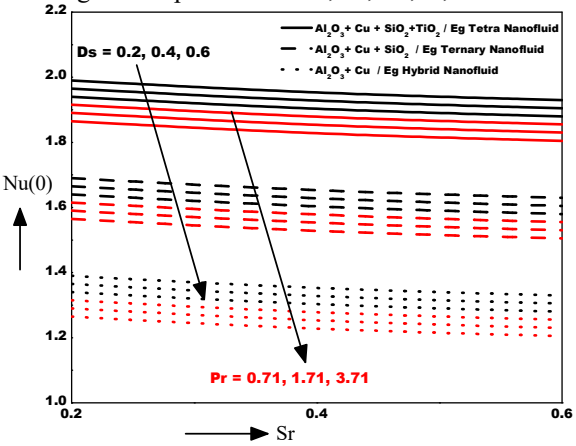


Fig.28 : Impression of Sr, Ds, Pr on Nu

Cover Page

INTERNATIONAL JOURNAL OF MULTIDISCIPLINARY EDUCATIONAL RESEARCH
ISSN:2277-7881(Print); IMPACT FACTOR :9.014(2025); IC VALUE:5.16; ISI VALUE:2.286
PEER REVIEWED AND REFEREED INTERNATIONAL JOURNAL
(Fulfilled Suggests Parameters of UGC by IJMER)
Volume:14, Issue:8(1), August, 2025
Scopus Review ID: A2B96D3ACF3FEA2A
Article Received: Reviewed : Accepted
Publisher: Sucharitha Publication, India
Online Copy of Article Publication Available : www.ijmer.in
https://doi.org/ijmer.in/14.08(1)/2025.33

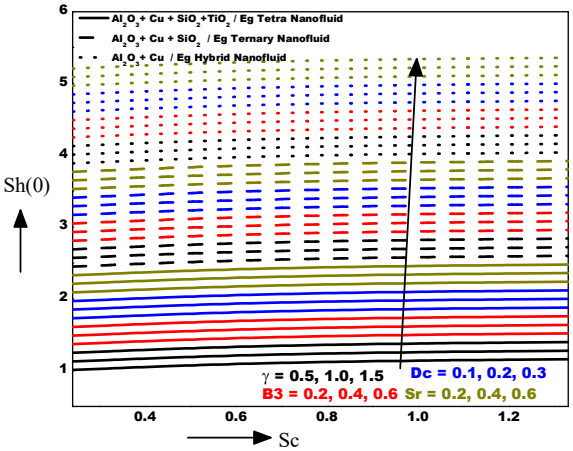


Fig.29 : Impact of Sc, γ, B3, Dc, Sr on Sh

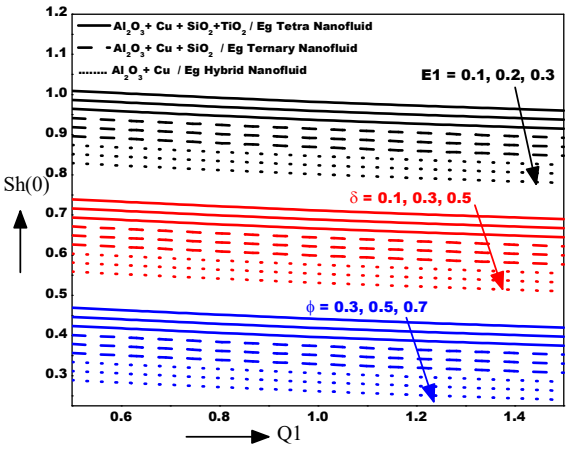


Fig.30: Control of Q1,Q, E1,δ, ϕ on Sh

10. REFERENCES

[1]. Bear, J. Dynamics of Fluids in Porous Media, Elsevier, New York, 1972.
[2]. Nield, D.A., ; and Bejan, A. Convection in Porous Medium, Springer, Verlag, New York, 2012.
[3]. Kvernvold, O.; and Tyvand, P., Journal of Fluid Mechanics, 99, 1980, 673-686.
[4]. Cheng, P., Letters in Heat and Mass Transfer, 8, 1981, 267-270.
[5]. Telles, R.S.; and Trevisan, O.V., International Journal Heat and Mass Transfer, 36(5), 1993, 1357-1365.
[6]. Hassanien, I.A.; Bakier, A.Y.,; and Gorla, R.S.R., Heat and Mass Transfer, 34, 1998, 209-212.
[7]. El-Hakiem, M.A., Transport in Porous Media, 45, 2001, 29-40.
[8]. Chamkha, A.J.,; Mujtaba, M.; and Quadri, A., Heat and Mass Transfer, 39, 2003, 561-569.
[9]. Khaled, A.R.A.; and Vafai, K., International Journal of Heat and Mass Transfer, 48, 2008, 2172-2185.
[10]. Ibrahim, A.A.; El-Amin, M.F.; and Salama, A., Forsch, Ingenieurwes, 72, 2008, 135-144
[11]. Mallikarjune B., Convective Heat and Mass Transfer in viscous fluid flow over a porous medium, Ph.D. Thesis submitted to J.N.T.U.A., Ananthapuramu, A.P., India, June, 2014.
[12]. Slattery J.C.. Momentum, energy and mass transfer in continua, Mc. Graw-Hill, New York, 1972.
[13]. Kristaiah Pallala : Effect of double dispersion on hydromagnetic convective heat and mass transfer flow past a vertical wavy wall with variable viscosity thermal conductivity, thermal radiation in the presence of temperature dependent heat sources, Ph.D. Thesis, A.P. Ambedkar Open University, Hyderabad, Talangana, India(2018)
[14]. Sreenivasa Reddy B and Ranganatha Reddy P : Effect of double dispersion on hydromagnetic convective heat and mass transfer flow past a vertical wavy wall with variable viscosity thermal conductivity, thermal radiation , chemical reaction in the presence of non-uniform heat sources, JXAT Journal , Vol.III, Issue – 4, April-2021, pp.281-295, ISSN No : 1006-7930 https://doi.org/10.37896/JXAT13.4/30727
[15]. Srinivasacharya D., Mallikarjuna B. and Bhuvanavijaya R., Soret and Dufour effects on mixed convection along a vertical wavy surface in a porous medium with variable properties, Ain Shams Engineering Journal, 6, (2015), 553-564.
[16]. Srinivasacharya, D.; Pranitha J.; and Ramreddy, Ch., International Journal for Computational Methods and Engineering Science and Mechanics, 13, 2012, 210-218.
[17]. Srinivasacharya. D, Bhuvanavijaya. R, and Mallikarjuna B.; Dispersion Effects on Mixed Convection over a Vertical Wavy Surface in a Porous Medium with Variable Properties, International Conference on Computational Heat and Mass Transfer,

Cover Page

INTERNATIONAL JOURNAL OF MULTIDISCIPLINARY EDUCATIONAL RESEARCH
ISSN:2277-7881(Print); IMPACT FACTOR :9.014(2025); IC VALUE:5.16; ISI VALUE:2.286
PEER REVIEWED AND REFEREED INTERNATIONAL JOURNAL
(Fulfilled Suggests Parameters of UGC by IJMER)
Volume:14, Issue:8(1), August, 2025
Scopus Review ID: A2B96D3ACF3FEA2A
Article Received: Reviewed : Accepted
Publisher: Sucharitha Publication, India
Online Copy of Article Publication Available : www.ijmer.in
https://doi.org/ijmer.in/14.08(1)/2025.33

Procedia Engineering, ELSEVIER, 127, 2015, 271-278

[18]. Amitosh Tiwari, D. R.V. Prasada Rao and G.N. Ramakrishna : Numerical Analysis of Dispersion and Activation Energy of Convective Heat Transfer Flow Past Wavy Surface with Variable Properties and Heat Sources, Journal of Technology, Vol.14(1), 2026, pp.329-341, ISSN: 10123407

[19]. Netai Roy and Dulal Pal, : Influence of Activation Energy and Nonlinear Thermal Radiation with Ohmic Dissipation on Heat and Mass Transfer of a Casson Nanofluid Over Stretching Sheet, *Journal of Nanofluids*, Vol. 11, No. 6, (2022) pp. 819–832, doi:10.1166/jon.2022.1882, www.aspbs.com/jon

[20]. Krishna M. V., Ahamad N. A., and Chamkha A. J., Hall and ion slip impacts on unsteady MHD convective rotating flow of heat generating/absorbing second grade fluid, 60, 845 (2021), DOI: 10.1016/j.aej.2020.10.013.

[21]. Devasena Y: Effect of non-linear thermal radiation, activation energy on hydromagnetic convective heat and mass transfer flow of nanofluid in vertical channel with brownian motion and thermophoresis in the presence of irregular heat sources, *World Journal of Engineering Research and Technology* (JERT) *wjert,* , *Vol. 9, Issue 2, XX-XX,* (2023) ISSN 2454-695X, SJIF Impact Factor: 5.924, www.wjert.org

[22]. Kathyani,G and Venkata Subrahmanyam,P:Effect of dissipation on HD convective heat and mass transfer flow of thermally radiating nanofluid in vertical channel with activation energy and irregular heat sources. *MukthShabd Journal*, (2023), ISSN No.2347-3150,Scientific Journal;ISSN No:2347-3150,Vol.XII,Issue.III, pp.433-441

[23]. Nagasasikala M : Effect of activation energy on convective heat and mass transfer flow of dissipative nanofluid in vertical channel with Brownian motion and thermophoresis in the presence of irregular heat sources, *World Journal of Engineering Research and Technology* (JERT) *wjert,* (2023)*, Vol. 9, Issue 2, XX-XX,* ISSN 2454-695X, SJIF Impact Factor: 5.924, www.wjert.org

[24]. Satya Narayana K and Ramakrishna G N : Effect of variable viscosity, activation energy and irregular heat sources on convective heat and mass transfer flow of nanofluid in a channel with brownian motion and thermophoresis, *World Journal of Engineering Research and Technology* (JERT) *wjert,* (2023)*, Vol. 9, Issue 2, XX-XX,* ISSN 2454-695X, SJIF Impact Factor: 5.924, www.wjert.org

[25]. Obalalu Adebowale Martins, Ajala Olusegun Adebayo, Adeshina Taofeeq Adeosun, Akintayo Oladimeji Akindele, Olayinka Akeem Oladapo, Olatunbosun Akintayo Olajide, Adegbite Peter : Significance of variable electrical conductivity on non-Newtonian fluid flow between two vertical plates in the coexistence of Arrhenius energy and exothermic chemical reaction, Partial Differential Equations in Applied Mathematics 4 (2021) 100184, https://doi.org/10.1016/j.padiff.2021.100184

[26]. Obalalu AM, Ajala AO, Akindele AO, Oladapo OA, Adepoju O, Jimoh OM. Unsteady squeezed flow and heat transfer of dissipative casson fluid using optimal homotopy analysis method: An application of solar radiation. *Partial Diff Equ Appl Math*. 2021:100146. http://dx.doi.org/10.1016/j.padiff.2021.100146.

[27]. Obalalu AM, Ajala OA, Abdulraheem A, Oladimeji AA. The influence of variable electrical conductivity on non-Darcian Casson nanofluid flow with first and second-order slip conditions. *Partial Diff Equ Appl Math*. 2021:100084. http://dx.doi.org/10.1016/j.padiff.2021.100084.

[28]. Adeshina T. Adeosun, Joel C. Ukaegbu: Effect of the variable electrical conductivity on the thermal stability of the MHD reactive squeezed fluid flow through a channel by a spectral collocation approach, Partial Differential Equations in Applied Mathematics 5 (2022) 100256, https://doi.org/10.1016/j.padiff.2021.100256

[29]. Jan, R. Nawaz, A. Ahmad, Non-similar analysis of radially magnetized flow and heat transfer of Reiner–Philippoff based nanofluid over a curved stretching surface with viscous dissipation, International Journal of Thermofluids 22 (2024) 100657.

[30]. Ramadhan AI, Azmi WH, Mamat R, Nanoscience. Nanotechnology-Asia. 2021;11(4):121–31. https://doi.org/10.2174/2210681210999200806153039

[31]. Vedavathi N, Dharmaiah G, Abdul Gaffar S, Venkatadri K. Entropy analysis of nanofluid magnetohydrodynamic convection flow past an inclined surface: a numerical review. Heat Transf. 2021;50(6):5996–6021. https://doi.org/10.1002/htj.22159.

[32]. Guedri K, Khan A, Sene N, Raizah Z, Saeed A, Galal AM. Thermal flow for radiative ternary hybrid nanofluid over nonlinear stretching sheet subject to Darcy–Forchheimer phenomenon. Math Probl Eng. 2022;2022:ArticleID3429439. https://doi.org/10.1155/2022/3429439.

[33]. Abbas W.Z. Adnan, M. Bani-Fwaz, Asogwa K. Kenneth, Thermal efficiency of radiated tetra-hybrid nanofluid [(Al2O3-CuO-TiO2-Ag)/water] tetra under permeability effects over vertically aligned cylinder subject to magnetic field and combined convection, Sci. Prog. 106 (1) (2023) 00368504221149797.

[34]. A.J.Chamkha,I.V.Miroshnichenko and M.A.Sheremet:Numerical analysis of unsteady conjugate natural convection of hybrid based nanofluid in a semicircular cavity.,Journal of Thermal Science and Engineering Applications,Vol.9,N0.4,Article ID.041004,(2017)

Cover Page

INTERNATIONAL JOURNAL OF MULTIDISCIPLINARY EDUCATIONAL RESEARCH
ISSN:2277-7881(Print); IMPACT FACTOR :9.014(2025); IC VALUE:5.16; ISI VALUE:2.286
PEER REVIEWED AND REFEREED INTERNATIONAL JOURNAL
(Fulfilled Suggests Parameters of UGC by IJMER)
Volume:14, Issue:8(1), August, 2025
Scopus Review ID: A2B96D3ACF3FEA2A
Article Received: Reviewed : Accepted
Publisher: Sucharitha Publication, India
Online Copy of Article Publication Available : www.ijmer.in
https://doi.org/ijmer.in/14.08(1)/2025.33

[35]. T.Gul and A.Saeed:Nonlinear mixed convection couple stress tri-hybrid nanofluids flow in a Darcy-Forchheimer porous medium over a non-linear stretching sheet ,Waves in Random and Complex Media,pp.1-18(2022)
[36]. T. Sajid, A.A. Gari, W. Jamshed, M.R. Eid, N. Islam, K. Irshad, G.C. Altamirano, S.M. El Din, Case study of autocatalysis reactions on tetra hybrid binary nanofluid flow via Riga wedge: biofuel thermal application, Case Stud. Therm. Eng. 47 (2023) 103058.
[37]. T. Hayat, Ambreen Safdar, M. Awais, S. Mesloub, Soret and Dufour effects for three-dimensional flow in a viscoelastic fluid over a stretching surface, Int. J. Heat Mass Transf. 55 (2012) 2129–2136.
[38]. Khan M, Rasheed A. Slip velocity and temperature jump effects on molybdenum disulfide mos_2 and silicon oxide sio_2 hybrid nanofluid near irregular 3D surface. Alex Eng J. 2021;60(1):1689–701. https://doi.org/10.1016/j.aej.2020.11.019.
[39]. Mingyu Z, Jing W. Effects of interfacial velocity or temperature slips on finite line contact thermal EHL in simple sliding motion. Tribology. 2024;44(8):1092–106. https://doi.org/10.16078/j.tribology.2023110.
[40]. Maranna T, Sachin GM, Mahabaleshwar US, Pérez LM, Shevchuk IV. Impact of navier's slip and MHD on a hybrid nanofluid flow over a porous stretching/shrinking sheet with heat transfer. Fluids. 2024;9(8):180. https://doi.org/10.3390/fds90801 80 .
[41]. Sarkar S, Mondal H, Kundu P. Artificial neural network prediction on negative and positive activation energy of magneto-hydrodynamic nanofluid flow with multiple slips. Hybrid Adv. 2025;100452. https://doi.org/10.1016/j.hybadv.2025.100452.
[42]. Prasun Choudhary, K. Loganathan, Kavita Jat, Krishna Prakash Arunachalam & S. Eswaramoorthi. Thermal and velocity slip impacts on MHD tetra-hybrid nanofluids flow over a porous stretching surface. *Discov Appl Sci* 7, 720 (2025). https://doi.org/10.1007/s42452-025-07359-6
[43]. B.K. Jha, A.O. Ajibade., Free convective flow of heat generation/absorption fluid between vertical porous plates with periodic heat input, Int. Commun. Heat Mass Trans. 36 (2009) 624–631.
[44]. B.K. Jha, A.O. Ajibade., Unsteady free convective Couette flow of heat generating/ absorbing fluid, Int. J. Energy Technol. 2 (12) (2010) 1–9.
[45]. S. Siddiqa, S. Asghar, M.A. Hossain, Natural convection flow over an inclined flat plate with internal heat generation and variable viscosity, Math. Comput. Model. 52 (2010) 1739–1751.
[46]. Abiodun O. Ajibade, M. Kabir Tafida, The combined effect of variable viscosity and variable thermal conductivity on natural convection couette flow, International Journal of Thermofluids, Volumes 5–6, 2020, 100036, ISSN 2666-2027, https://doi.org/10.1016/j.ijft.2020.100036.
[47]. Agarwal P, Jain R, Loganathan K. Thermally radiative flow of MHD powell-eyring nanofluid over an exponential stretching sheet with swimming microorganisms and viscous dissipation: a numerical computation. Int J Thermofluids 2024;23: 100773. https://doi.org/10.1016/j.ijft.2024.100773.
[48]. Zegeye GB, Haile E, Awgichew G. Viscous dissipation and Joule heating effects of Carreau nanofluid axisymmetric flow past unsteady radially stretching porous disk. Int J Thermofluids 2024;22:100655. https://doi.org/10.1016/j.ijft.2024.100655.
[49]. Panda S, Ontela S, Thumma T, Mishra SR, Pattnaik PK. Mechanism of heat transfer in Falkner–Skan flow of buoyancy-driven dissipative hybrid nanofluid over a vertical permeable wedge with varying wall temperature. Mod Phys Lett B 2024;38 (1):2350211. https://doi.org/10.1142/S0217984923502111.
[50]. Kausar MS, Hussanan A, Qasim M, Mamat M. Flow of water based nanofluid containing different shapes of Cu nanoparticles embedded in a porous medium. Int J Appl Comput Math. 2021;7(3):107. https://doi.org/10.1007/s40819-021-01042-1.
[51]. Grubka LJ, Bobba KM. Heat transfer characteristics of a continuous stretching surface with variable temperature. J Heat Transf. 1985;107(1):248–50. https://doi.org/10.1115/1.3247387.
[52]. Amudhini M, De P. Soret-Dufour driven unsteady MHD bioconvective tetra-hybrid nano-additives over rotating disks with varying thermophysical property. Results Eng. 2025;25:103828. https://doi.org/10.1016/j.rineng.2024.103828.
[53]. Sajid T, Algarni S, Ahmad H, Alqahtani T, Jamshed W, Eid MR, Amjad A. Exploration of irreversibility process and thermal energy of a tetra hybrid radiative binary nanofluid focusing on solar implementations. Nanotechnol Rev. 2024;13(1):20240040. https://doi.org/10.1515/ntrev-2024-0040.
[54]. Seddeek,M.A and Salem,A.M: Laminar mixed convection adjacent to vertical continuously stretching sheet with variable viscosity and variable thermal diffusivity, Int. J. Heat and Mass transfer,V.41,pp.1048-1055(2005).
[55]. E. Magyari and B. Keller, "Heat and mass transfer in the boundary layers on an exponentially stretching continuous surface," Journal of Physics D: Applied Physics 32 (1999) doi: 10.1088/0022-3727/32/5/012.
[56]. Bhattacharya,K and Layek,G.C: Mgnetohydrodynamic boundary layer flow of nanofluids over an exponentially stretching permeable sheet.Hindawi Publishing Corporation Physis Research International V.2014Article ID 59253612 pages(2014)